S-1 MPC

Sentinel-1 Ocean Swell Wave Spectra (OSW) Algorithm Definition

Chronology Issues:

Issue:	Date:	Reason for change:	Author
1.0	09/08/2010	First version	H.Jonhsen, F.Collard
1.1	08/11/2010	Added comment to the *lowpass* routine Renamed variables in Table 4 Clarified the Internal Processing File text Added clarification to Figure 13 and Figure 14. Added reference to Figure 14. Updated Figure 2 and Figure 3 with explicit auxiliary file specifications Added input and output parameters for each module (steps) Redistributed the processing steps to comply with the flowcharts Added new quality measured to output product list. Included new Section 3 describing the L2 OCN processing context Addressed the following minor RIDS: S1IPFPDR-266, S1IPFPDR-267, S1IPFPDR-268, S1IPFPDR-269, S1IPFPDR-271.	H.Jonhsen, F.Collard
1.2	27/04/2011	Updated the flowcharts, Figure 3 and Figure 6. Added Table 1 and Table 2. Addressed the RIDS S1IPFPDRL2-1, S1IPFPDRL2-6, S1IPFPDRL2-8, S1IPFPDRL2-9, S1IPFPDRL2-10, S1IPFPDRL2-11, S1IPFPDRL2-12, S1IPFPDRL2-13, S1IPFPDRL2-32.	H.Jonhsen, F.Collard
1.3	16/09/2019	Introducing quality flag and Normalized Standard deviation variables, updating information an integral parameters estimation, low frequency removal and partitioning Update the template of the document. Introduction: Clarify the scope of this document	R.Husson G.Hajduch

People involved in this issue:

Written by(*):	R.Husson and P.Vincent	
Checked by(*):	G.Hajduch	G.Hajduch
Approved by(*):	G.Hajduch	G.Hajduch

*In the opposite box: Last and First name of the person + company if different from CLS

Index Sheet:

Context:	Sentinel-1 Mission Performance Center
Keywords:	Sentinel-1, Instrument Processing Facility, ATBD, Swell measurement

Distribution:

Company	Means of distribution	Names
ESA	Electronic	N.Miranda

List of tables and figures

List of tables:

List of figures:

List of Contents

1. Introduction

1.1. Purpose

The objective of this document is to define and describe the algorithm implemented in the S1 L2 IPF and the processing steps for the generation of the Ocean Swell Spectra (OSW) component of the Sentinel-1 Level 2 Ocean (OCN) product.

1.2. Scope

The OCN product contains three sub-products: the OSW component, the Ocean Wind Field (OWI) component, and the Radial Surface Velocity (RVL) component. These three components are all merged into a common OCN product for the Wave Vignette (WV) and Stripmap (SM) modes. For TOPS (IW and EW) modes the L2 OCN product contains the OWI and RVL components only. A description on how all these three components (OSW, OWI, RVL) are connected into the L2 ocean processing can be found in Section 3. However, this document contains only the OSW algorithm definition. The OWI and RVL algorithm definitions are provided in separate documents [A-9], [A-10].

The versions 1.0 to 1.2 of this document were prepared by NORUT and CLS as part of the development of the Level 2 processing part of the IPF.

The next versions of this document were prepared by CLS as part of the maintenance and evolutions of the S-1 IPF

This document satisfies the PAL2-1 deliverable defined as per the content defined in the Sentinel-1 IPF Statement of Work [A-1] for review at the Sentinel-1 IPF Preliminary Design Review (PDR L2) and Critical Design Review (CDR L1 & L2).

1.3. Document Structure

This document is structured as follows:

• Section 1 introduces the purpose, scope, structure and conventions of the document.

• Section 2 lists the applicable and reference documents.

• Section 3 gives a contextual overview of the L2 OCN product

• Section 4 gives a short L2 OSW component overview

• Section 5 gives the L2 OSW processing system overview

• Section 6 details the functional description of the various processing units

• Section 7 describes the auxiliary input data and parameter files

• Section 8 lists key symbols used in the document

• Section 9 lists the content of the OSW output NetCDF file

2. Documents

2.1. Applicable Documents

A-1   GMES-DFPR-EOPG-SW-07-00006   Sentinel-1 Product Definitions & Instrument Processing Facility Development Statement of Work, Issue/Revision 4/1, 23-05-2008.

A-2   Contract Change Notice N.2, Changes in ESRIN Contract No. 21722/08/I_LG, June 21, 2010

A-3   DI-MPC-PB-0241 Sentinel-1 IPF Auxiliary Product Specification, Issue/Revision 3/4 Jan. 07, 2020

A-4   S1-RS-MDA-52-7441, Sentinel-1 Product Specification, Issue/Revision 3/7, Feb. 27, 2020

A-5   SEN-RS-52-7440, Sentinel-1 Product Definition, Issue/Revision 2/3, Mar. 28, 2011

A-6   01-4709-2   MDA Consolidated Final Proposal to the European Space Agency for Sentinel-1 Products Definition and Instrument Processing Facility Development. June 12, 2008. MacDonald Dettwiler.

A-7   Johnsen H., Engen G., Collard F., Chapron B., "Envisat ASAR Level 2 Wave Mode Product Algorithm Specification – Software Requirements Document", Norut Report No. IT650/1-01, v.2.3.0, 24 Oct. 2006

A-8   Collard F., Johnsen H., "SAR Ocean Wind Waves And Currents – Software Requirements Document", CLS Report No. BO-024-ESA-0408-SRD-2 waves, v.1.2, Nov.2006

A-9   [S1-AD-21]-S1-TN-CLS-52-9049   Sentinel-1 Ocean Wind Field (OWI) Algorithm Definition, Issue/Revision 2.0, June.27, 2019, CLS.

A-10   S1-TN-NRT- 53-0658 Sentinel-1 L2 Doppler and Ocean Radial Velocity (RVL) Algorithm Definition, Issue/Revision 1/2, May 6, 2011, NORUT.

A-11   http://www.unidata.ucar.edu/software/netcdf/

A-12   S1-IC-MDA-52-7454   Sentinel-1 Instrument Processing Facility Interface Control Document, Issue/Revision 1/3, Apr. 9, 2011, MDA.

2.2. Reference Documents

The following documents provide useful reference information associated with this document. These documents are to be used for information only. Changes to the date/revision number (if provided) do not make this document out of date.

R-1   ES-RS-ESA-SY-0007   Mission Requirements Document for the European Radar Observatory Sentinel-1, Issue 1/4, ESA, July 11, 2005

R-2   Lotfi A., Lefevre M., Hauser D., Chapron B., Collard F., "The impact of using the upgraded processing of ASAR Level 2 wave products in the assimilation system", Proc. Envisat Symposium, 22-26 April 2007, Montreux

R-3   Kerbaol V., et al., "SAR Ocean Wind, Waves and Currents : Final Report and Executive Summary", Esrin/Conract NO 18709/05/I-LG, Ref. BO-024-ESA-0408-RF, v.2.0, 15 November 2006

R-4   BOOST Technologies, SAR WINDS WAVES CURRENTS Validation technical notes, Technical note (WP6), BO-024-ESA-0408-VTN, version 1.0, 09/08/2006

R-5   Kerbaol V., Johnsen H., "Technical Support for Global Validation and Long-Term Quality Assessment and Optimization of ASAR Wave Mode Products: Cycle Reports", http://www.boost-technologies.com/web/

R-6   Chapron B., Collard F., Ardhuin F., "Direct measurements of ocean surface velocity from space: Interpretation and validation", Journal of Geophysical Res., 110, C07008, 2005

R-7   Horstmann J., "Measurements of Ocean Wind Fields with Synthetic Aperture Radar", University of Hamburg, Faculty of Earth Sciences, 2002, external GKSS report, GKSS 2002/5, ISSN 0344-9629, 2002

R-8   Mouche A.A., Chapron B., Reul N., Collard F., "Predicted Doppler shifts induced by ocean surface wave displacements using asymptotic electromagnetic wave scattering theories", Waves in Random and Complex Media, Volume http://www.informaworld.com/smpp/title%7Econtent=t716100762%7Edb=all%7Etab=issuesli st%7Ebranches=18 - v1818, Issue 1 February 2008 , pages 185 – 196

R-9   Collard F., Chapron B., Johnsen H., "Sentinel-1 SAR Wave Mode", Technical Note, Boost Technologies, v1.0, Dec 2007.

R-10   Johnsen H., Engen G., Guittion G., "Sea-Surface Polarisation Ratio from Envisat ASAR AP Data", IEEE Trans. on Geo. Rem. Sensing, Vol.46, No.11, Nov. 2008.

R-11   Ardhuin F., A. D. Jenkins, D. Hauser, A. Reiers, B. Chapron, "Waves and Operational Oceanography: Toward a Coherent Description of the Upper Ocean", Eos, Vol.86, No.4, 25 January 2005

R-12   Engen G., Pedersen I. F., Johnsen H., Elfouhaily T., "Curvature Effects in Ocean Surface Scattering", IEEE Trans. on Antennas and Propagation, Vol.54, No.5, May, 2006.

R-13   Goldfinger A. D., "Estimation of Spectra From Speckled Images", IEEE Trans. on AeroSpace and Electronic Systems, Vol. AES-18, No.5, 1982.

R-14   Engen G., Johnsen H., "A New Method for Calibration of SAR Images", Proc. of CEOS SAR Workshop, 26-29 Oct., Toulouse, 1999.

3. OCN Product Overview

The level-2 (L2) ocean product (OCN) has been designed to deliver geophysical parameters related to the wind, waves and surface velocity to a large panel of end-users. The L2 OCN products are estimated from Sentinel-1 (S-1) Synthetic Aperture Radar (SAR) level-1 (L1) products.

L2 OCN products are processed by the level 2 IPF processor and benefit from robust and validated algorithms [R-4]. A diagram of the L2 Ocean processing unit context is presented in Figure 1. In this figure, external IPF interfaces have a white background, internal IPF interfaces are identified by a grey background, and interfaces with a yellow background are only applicable when the L2 processor is used in test mode outside of the normal IPF environment.
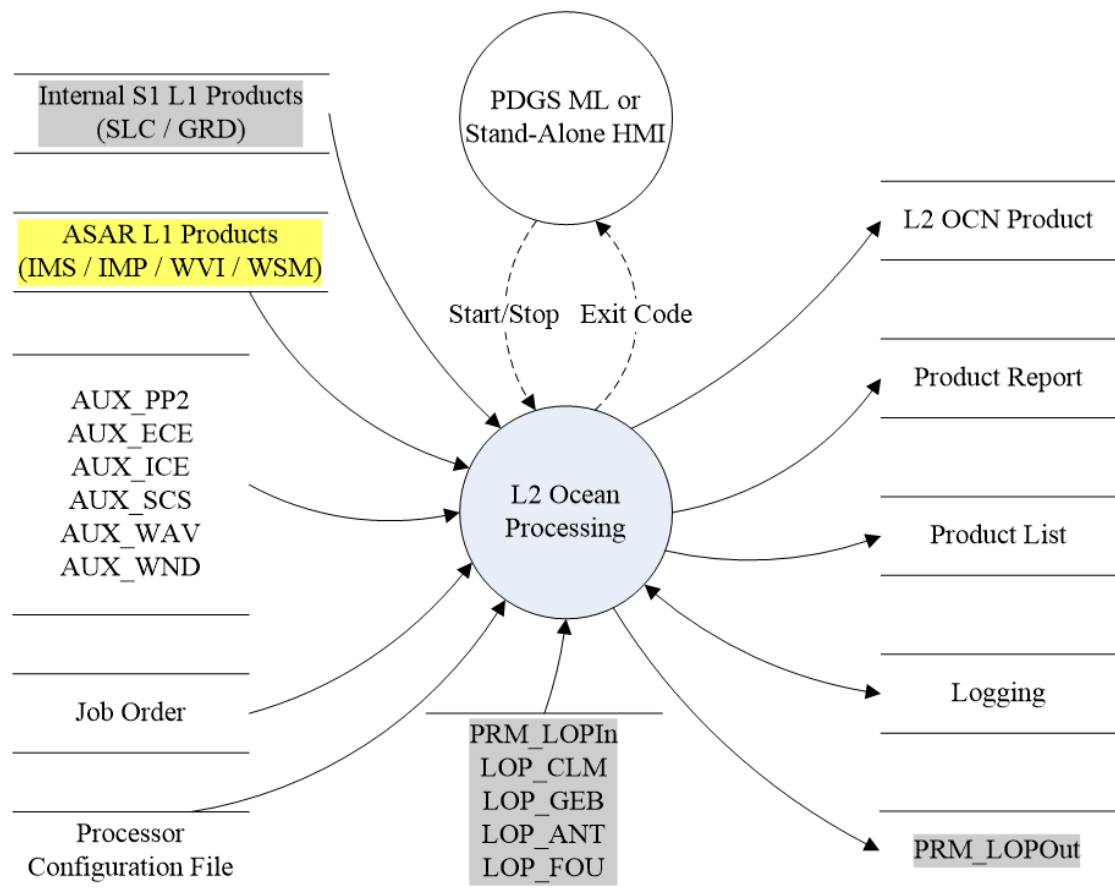
Figure 1 : Sentinel-1 L2 Ocean Processing Context Diagram

The processor can be used in PDGS environment or in a stand-alone HMI mode. In both cases, a job order is read by the processor to get all high-level information required for processing a particular product (e.g. names and directories of input L1 files, names and directories of auxiliary data files, directories of outputs files, etc…). Processing then starts from L1 products using the auxiliary data files provided (e.g. the L2 processor parameter file). During the processing, a log file is generated to monitor the status of each processing step. The final step of the processing is the creation of the product including writing of all the geophysical information into NetCDF files.

3.1. Product Organisation

Each L2 OCN product contains up to three geophysical components: the radial velocity (RVL), the ocean surface wind field (OWI) and the ocean swell wave spectra (OSW) components. These components are formatted into one output NetCDF file. For SM and WV modes, the L2 product contains all three components. For TOPS mode, the product contains only RVL and OWI components. The detailed algorithm definition of each component is described in a dedicated document (This document is for OSW and [A-9],[A-10] are for OWI and RVL). The outputs variables related to each component are listed and defined in the product definition document [A-5].

For the SM and TOPS modes, the information related to each component is estimated onto a specific grid cell (ground range) whose properties are chosen to optimize the inversion schemes. As a consequence, the SM mode output NetCDF file has three components and the TOPS mode output NetCDF file has two components, each set having its own resolution. In addition, the most pertinent geophysical parameters from RVL and OSW components are interpolated onto the OWI grid to get a set of variables defined at the same resolution. The default value for the resolution of this common grid is 1 km for SM and TOPS modes. The set of variables from RVL and OSW interpolated onto OWI grid is listed in section 8 of the OWI document [A-9]. RVL and OSW are estimated from L1 SLC internal product. OWI is estimated from L1 GRD internal product.

For WV mode, there is no grid. In this case, the resolution of the components is simply the size of the imagette: 20 km. The three components are estimated from L1 SLC internal products.

3.2. Processing Workflow

For SM and TOPS modes, the components are estimated independently. This means that for a given acquired scene, the steps for each component are:

- the appropriate L1 internal product is read,
- the variables corresponding to the considered component are estimated
- a temporary file containing the results is saved locally.

For each component, these three latter steps are executed by different IDL scripts based on the same library of IDL functions. These three scripts are coordinated by a Python script which collects all information mandatory for L1 processing of each component. Then, when it is completed for all components, the components outputs are merged into a single NetCDF. The same way, for each type of file generated by the three independent scripts, a merging is done.

For WV mode, the three components are estimated sequentially from the same L1 SLC internal product with the same IDL script.

The SM and TOPS modes have the dual-polarization option. However, the L2 OCN components are always estimated only using the information from the co-polarized signal. Thus, the algorithms for each component as well as the workflow for the L2 OCN product generation are not different from that of single polarization product.

The OCN Product consists of three components (OWI, OSW and RVL), and these three components are derived through three different processing algorithms:

- The Ocean Swell Spectra algorithm, as described by this document.
- The Ocean Wind Field algorithm, as described in A-9.
- The L2 Doppler Grid algorithm, as described in A-10.

Table 1 presents a summary of which components are included in the OCN Product per acquisition mode, the L2 processing algorithm used to calculate the values for that component, and the type of input L1 product (either SLC or GRD) is required by each algorithm. Further details about these L1 GRD and SLC L1 products can be found in the respective algorithm documents (see section 7.3 of this document for the Ocean Wind Field algorithm L1 inputs).

Table 1 : L2 OCN Product Content and Processing Algorithm per Acquisition Mode

Acquisition Mode	L2 OCN Product Component	Input L1 Product	L2 Processing Algorithm		
			Ocean Swell Spectra Algorithm	Ocean Wind Field Algorithm	L2 Doppler Grid Algorithm
SM	OSW	SLC	✓		
	OWI	GRD		✓	
	RVL	SLC			✓
IW	OWI	GRD		✓	
	RVL	SLC			✓
EW	OWI	GRD		✓	
	RVL	SLC			✓
WV	OSW	SLC	✓		
	OWI	SLC	✓		
	RVL	SLC			✓

The L2 processing algorithms support the processing of both Sentinel-1 and ASAR L1 products that have been produced by the S1 IPF in the Stand-Alone environment. In the Test Mode of the L2 OCN Processor, they can also use L1 products that have been produced by the PF-ASAR processor, and therefore follow the ENVISAT/ASAR product format. Table 2 shows the acquisition modes, sensors and input product types supported by each of the three L2 processing algorithms.

Table 2 : Input L1 Products Supported by L2 Processing Algorithms

L2 Processing Algorithm	Acquisition Mode	Sensor	L1 Processor	L1 Product Type
Ocean Swell Spectra	SM	Sentinel-1	S1 IPF	SLC
		ASAR	S1 IPF	SLC
		ASAR	PF-ASAR	IMS
	WV	Sentinel-1	S1 IPF	SLC
		ASAR	S1 IPF	SLC
		ASAR	PF-ASAR	WVI
Ocean Wind Field	SM	Sentinel-1	S1 IPF	GRD-MR
		ASAR	S1 IPF	GRD-MR
		ASAR	PF-ASAR	IMP
	IW	Sentinel-1	S1 IPF	GRD-MR
	EW	Sentinel-1	S1 IPF	GRD-MR
	WS	ASAR	PF-ASAR	WSM
L2 Doppler Grid	SM	Sentinel-1	S1 IPF	SLC
		ASAR	S1 IPF	SLC
		ASAR	PF-ASAR	IMS
	WV	Sentinel-1	S1 IPF	SLC
		ASAR	S1 IPF	SLC
		ASAR	PF-ASAR	WVI
	IW	Sentinel-1	S1 IPF	SLC
	EW	Sentinel-1	S1 IPF	SLC

4. OSW Component Overview

The Sentinel-1 SAR can be operated in one of four nominal acquisition modes:

- Stripmap Mode (SM)
- Interferometric Wide-swath Mode (IW)
- Extra-Wide-swath Mode (EW)
- Wave Mode (WV)

The Sentinel-1 wave retrieval processing supports the following two instrument modes:

- Stripmap Mode (SM) (co-polarized channel)
- Wave Mode (WV)

The Sentinel-1 Level 2 OSW component of the OCN product is the two-dimensional ocean surface wave spectra estimated from a Sentinel-1 Level 1 Single-Look Complex (SLC) SAR image by inversion of the corresponding image cross-spectra. The cross spectra are computed by performing inter-looking in azimuth followed by co- and cross-spectra estimation among the detected individual look images. The image from which a single OSW is computed can be a SLC imagette from the WV mode, or a co-polarized sub-image extracted from a SM SLC image.

The spatial coverage of one cell of the OSW component is equal to the spatial coverage of the corresponding L1 WV-SLC or sub-images extracted from the L1 SM-SLC product. It is limited to ocean areas.

The OSW component is given on log-polar grid for the wavenumber [rad/m] and direction [degN] in units of [m4]. The spatial and spectral resolutions depend on the mode of the SAR instrument. Because of the nature of SAR ocean wave imaging, the actual spectral resolution also depends on the direction of wave propagation relative to azimuth and the sea state.

The OSW component contains additional parameters derived from the ocean wave spectra (integrated wave parameters) and from the imagette (image statistics). It includes also an estimate of the wind sea significant wave height [m]. Some key sensor parameters from the L1 product from which the OSW component is generated are also included in the product.

The Terrain Observation with Progressive Scans SAR (TOPSAR) mode is not optimal for OSW component generation since individual looks with sufficient time separation are required. The inter-look time separation obtained within one burst is too short due to the progressive scanning (i.e. short dwell time). Individual looks from neighboring bursts require significant spatial overlap. This is not obtained with the standard configurations of the TOPS mode.

5. General Description

The Sentinel-1 wave processing system consists of a spectral estimation unit followed by a spectral inversion unit. The spectral estimation unit performs the processing from Level 1 SLC product to an internal co- and cross-variance function (Level 1b) product, which optionally can be stored as an internal output product. The spectral inversion unit generates the Level 2 OSW product using the intermediate Level 1b data product as input. In the algorithm the intermediate product will not be stored in a separate file but will be kept in the memory during the processing. The OSW processing unit is integrated with the OWI and RVL processing units to produce the OCN product. This means that they share the same basic library, and the functionalities are compatible. Figure 2 below presents the main high-level SAR wave retrieval processing units with their input and output data. The OSW component (NetCDF) will be merged with the corresponding OWI and RVL components to form the OCN Product NetCDF file as described in Section 3.

External Data
- SAR SLC Products
- Auxiliary Data

OSW- Spectral Estimation Unit

- Generation of Level 1b (Co- and Cross- Variance) Data on Internal Format (Section 5.1)

OWI unit
RVL unit

OSW – Spectral Inversion Unit
- Generation of OSW component from the Level 1b product
- Writing the OSW component into S-1 L2 format (Section 5.2)
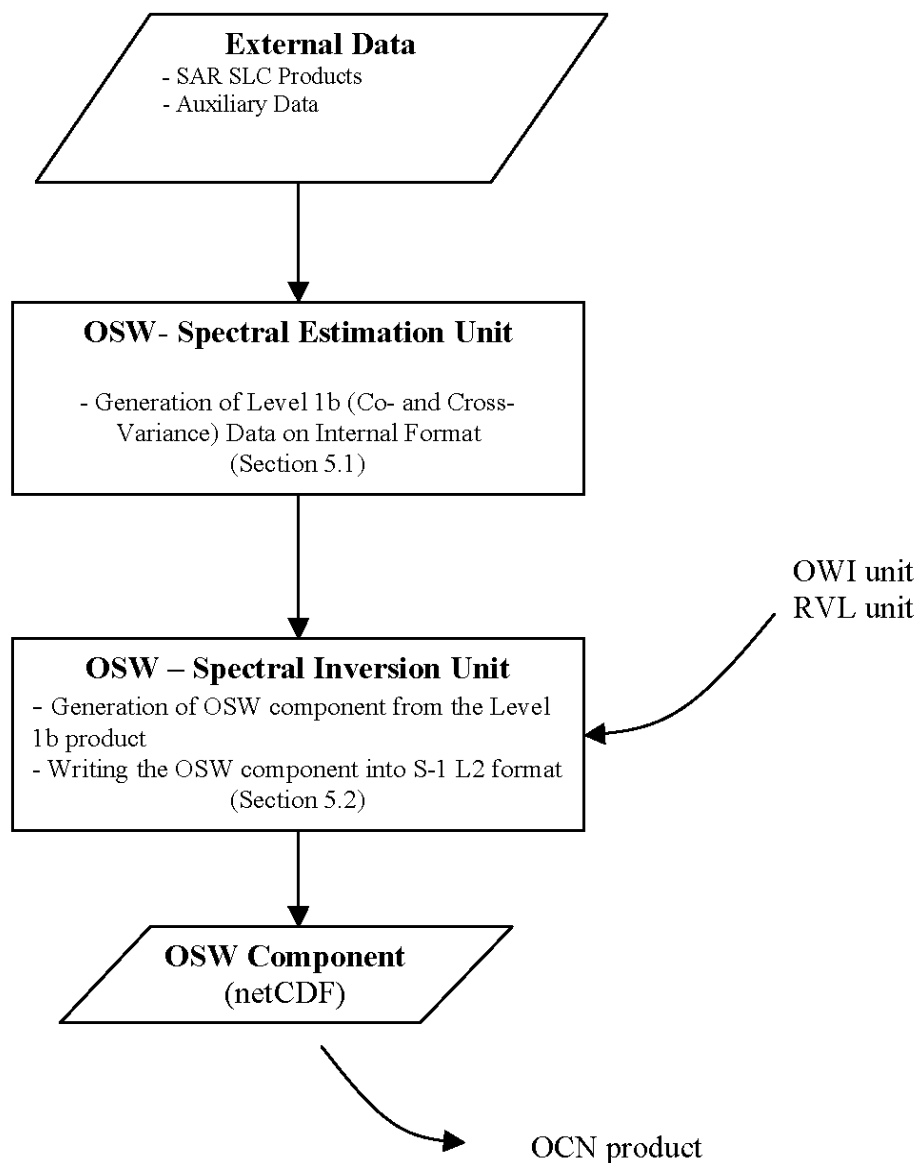
OSW Component
(netCDF)

OCN product

Figure 2 : High Level OSW Processing Algorithm

The OSW processing system will access the following inputs:

1. A SAR image product and annotations as described in Section 7.3.1, which can be:
    - Sentinel-1 formatted product:
        - Internal S1 SLC SM or VW product
        - ASAR IM or WV simulated product
    - ASAR formatted product in either of the ASAR modes

2. External auxiliary data:
    - ECMWF Atmospheric Model Data, as described in Section 7.1.1
    - L2 Processor Parameters Auxiliary Data, as described in Section 7.1.2
    - Simulated Cross-Spectra Data, as described in Section 7.1.3

3. Internal auxiliary data:
    - Coastline and Land Masking Data, as described in Section 7.2.1
    - General Bathymetry Chart of the Oceans (GEBCO)(in case of SM data), as described in Section 7.2.2
    - Range Fourier profile, as described in Section 7.2.3
    - IPF L2 internal parameter file contains extra processing parameters specific to the OSW algorithm as described in Section 7.2.4 (and not specified in the Processor Parameters Auxiliary Data File).

The L2 processor will generate the OCN product as specified in the Sentinel-1 product specification format, this contains a NetCDF) with the L2 information. Optionally, the system (prototype) can also dump out the intermediate product (Level 1b) as an XML file. This intermediate output product is the co- and cross-variance function on full resolution cartesian grid with an info structure specifying the data content and origination. A 2D Fourier transform of these data will give the co- and cross-spectra on cartesian wavenumber grid.

5.1. Spectral Estimation Unit Overview

The OSW spectral estimation unit, leading to the internal intermediate product, consist of inter-look cross spectral processing based on splitting the azimuth bandwidth into three non-overlapping looks, followed by an estimation of the co- and cross-variance function based on the periodogram method. The final result consists of one co-variance function and two cross-variance functions on cartesian grid. The two cross-variance functions correspond to the neighbour looks and the outer looks i.e. with two different look separation times. The co-variance function is the average of the co-variance functions from the three individual looks. The processing unit also estimate the percentage of land within the selected estimation area (in case of SM data), the range and azimuth cut-off wavelength, spectral resolution, and some image statistics (mean, variance, skewness). This intermediate product is on cartesian grid in SAR coordinates and can optionally be written to an XML file.

5.2. Spectral Inversion Unit Overview

The OSW spectral inversion unit first accesses the intermediate product and perform a 2D Fourier transform to achive the co- and cross-spectra on cartesian grid. A Hanning windowing is used in doing the 2D Fourier transform, where the windowing parameter (i.e order of Hanning) is described in the internal processing parameter fil (Table 3). The OSW processing then performs a wave spectral inversion of the co- and cross-spectra with respect to the detected SAR ocean wave like pattern. This is done by first estimating and removing the non-linear contribution to the imaging

process assuming that this is caused only by the local wind field, and then to apply a quasi-linear inversion in the most energetic part of the SAR co- and cross-spectrum. The wind field is thus required, and this is estimated as described in the OSW processing.

A new feature as compared to the existing ASAR WM processing, is the estimation of wind sea significant wave height. This is performed using the estimated wind speed and the azimuth cut-off wavelength.

The major requirements for the quality of the inversion is knowledge of the Real Aperture Radar (RAR) Modulation Transfer Function (MTF), the azimuth cut-off wavelength, and an accurate removal of the non-linear part of the spectra (i.e. the wind field). The RAR MTF is computed using a backscattering model including non-uniform distribution of scatterers on the long wave field. The RAR MTF amplitude is provided in a simulated cross-spectra look-up table described in [Section 7.1.3]. After the inversion, the ocean wave spectrum is converted to polar grid, rotated relative to north, partitioned, and ambiguity resolved followed by computation of key spectral parameters for the two most energetic partitions. Finally, an output product is generated from the polar spectra and stored in a NetCDF format together with extracted parameters stored as attributes and some key parameters from the corresponding L1 product.

6. Functional Description

6.1. OSW – Spectral Estimation Unit

The spectral estimation unit extracts a sub-image from the L1 SLC image product and estimates the co- and cross-spectra. The estimation is repeated over the number sub-image calculated using the information provided in the processing parameter file [Table 1 : L2 OCN Product Content and Processing Algorithm per Acquisition Mode, Section 7.1.2] and in the internal parameter file [Table 5 : OSW – Internal processing parameter file, Section 7.2.4]. The spectral estimation unit is the same as used in the ASAR WM Level 2 processing [A-7].

6.1.1. Flowchart

Figure 3 shows the flowchart of the spectral estimation unit.
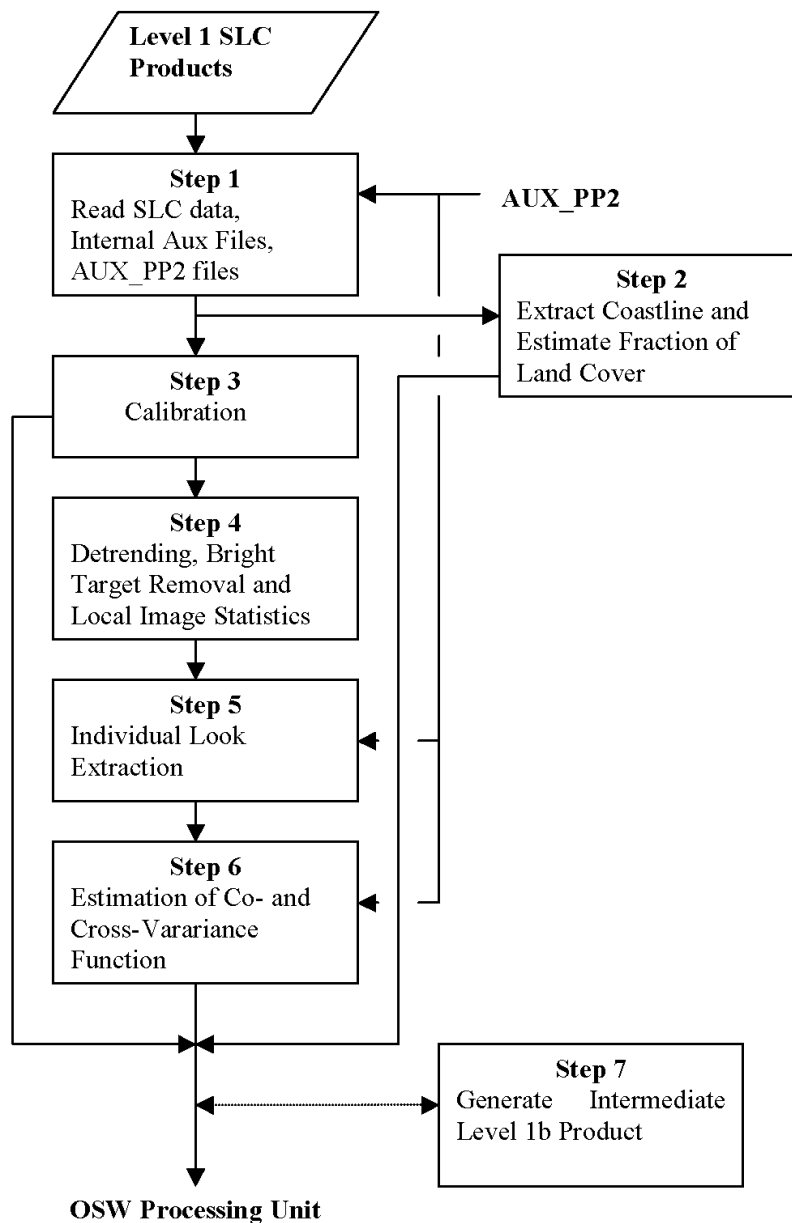
Figure 3 : Spectral Estimation Unit

6.1.2. Function and Purpose

The different processing steps in the flowchart are described below.

Step 1: Read SLC and AUX_PP2 data

Input Data: Level 1 SLC product, AUX_PP2 data, Internal Processing Parameter File

Output Data: SLC image (I_c)

The SLC reader object is initialized with the specified input Level 1 SLC product name and file path. The processing parameter information (see 0, Section 7.1.2) given in the processor auxiliary data and the internal processing (see 0, Section 7.2.4) file are accessed.

Step 2: Extraction of Coastline

Input Data: SLC image (I_c) , LOP_CLM file, Internal Processing Parameters

Output Data: Land flag

If the keyword for use of land mask data is set in the internal processing parameter file (Table 3) the following operations are performed:

- The coastline mask within the same geographic area as the imagette is extracted from the coastline and land masking file (see Section 7.2.1)
- The coastline mask is used to compute the percentage of land within the imagette. This is computed by reading the coordinate of a coastline polyline, converting the geo-coordinate of this polyline into image coordinate and then plotting the polyline contour in the IDL Z buffer (virtual screen) and fill the interior with a constant value.
- The land flag in output product is set if the percentage of land coverage within the estimation cell exceeds 10%.

Step 3: Calibration

Input Data: SLC image (I_c)

Output Data: Calibrated SLC image (I_c) , NRCS (σ_o)

Apply the Level 1 calibration vectors to remove the application LUT if necessary and to achieve absolute calibrated data. The LUT is part of the Level1 product [A-3].

Step 4: Detrending, Bright Target Removal and Computation of Local Image Statistics

Input Data: Calibrated SLC image (I_c) , Internal Processing Parameters

Output Data: Detrended SLC image (I_c), local image statistics (Mean (μ), Normalized variance ($\bar{\sigma}$), Skewness (β_s), Curtosis (β_k)

The bright target removal and the detrending remove ship and low frequency (no-wave) signatures in the complex image, I_c, respectively. This is necessary before doing the spectral estimation and higher order image statistics. The procedures are described in the following followed by procedures for computing local image statistics.

Detrending:

This is done by first generating a lowpass filtered version of the corresponding intensity image:

(1) $$I_{LP} = lowpass(|I_c|^2, w_x, w_y)$$

where the range and azimuth filter widths are given, respectively as:

(2) $$w_x = \frac{2 f_{sf} w \sin\theta}{c}$$

(3) $$w_y = \frac{f_{prf} w}{v_g}$$

The detrended SLC image is then given by reassigning and preserving the image intensity as:

$$I_c := I_c \sqrt{\frac{\mu_I}{I_{LP}}}$$
(4)

where μ_I is the mean image intensity of the input SLC image.

Here

w	= configurable filter parameter
f_{sf}	= range bandwidth [Hz]
f_{prf}	= pulse repetition frequency [Hz]
θ	= incidence angle [rad]
v_g	= radar ground velocity [m/s]

The configurable filter parameter is provided by the internal parameter file specified in Table 5 of Section [7.2.4]. The lowpass filter routine is a standard IDL library routine. The SAR parameters are extracted from the SLC product or computed using information from the SLC product (Table 5).

Bright Target Removal:

The bright target removal sets all pixels of the original complex image with normalized variance above certain threshold, equal to the values of the low pass filtered image, keeping the phase unchanged:

$$I_c(x_i,y_i) = \sqrt{I_{LP}(x_i,y_i)}\, e^{j\Phi(x_i,y_i)}$$
(5)

where

(x_i,y_i)	= bright target pixel (range,azimuth)
Φ	= phase of the original complex image.

Local Image Statistics:

The following formulas are used to compute the image statistics (mean intensity=μ, normalized variance=$\hat{\sigma}$, skewness=β_s, curtosis=β_k) from a complex image, I_c:

$$\mu = \left\langle |I_c|^2 \right\rangle$$
(6)

$$\hat{\sigma} = \frac{1}{\mu^2}\left\langle \left(|I_c|^2 - \mu\right)^2 \right\rangle$$
(7)

$$\beta_s = \frac{\left\langle \left(|I_c|^2 - \mu \right)^3 \right\rangle^2}{\left\langle \left(|I_c|^2 - \mu \right)^2 \right\rangle^3}$$

(8)

$$\beta_k = \frac{\left\langle \left(|I_c|^2 - \mu \right)^4 \right\rangle}{\left\langle \left(|I_c|^2 - \mu \right)^2 \right\rangle^2}$$

(9)

where < > denotes spatial averaging over the sub-image from where the spectra will be estimated.

Step 5: Individual Look Extraction

Input Data: Calibrated and Detrended SLC Image (I_c), AUX_PP2 parameters, Internal Auxiliary File (Range Fourier Profile)

Output Data: Three Individual Look Intensity Images ($I^{(m)}, m = 1,2,3$)

This procedure is identical to what is implemented and described for ASAR WM [**Erreur ! Source du renvoi introuvable.**]. The individual look extraction process is performed in the azimuth frequency domain after first equalizing the Fourier domain by removing the range and azimuth instrument functions. In azimuth direction this is done by removing the antenna function and windowing function (if any) applied to the data during the SAR processing. The azimuth Fourier profile is fully predictable and can be computed as:

$$Y(\underline{k}_y) = h_m(k_y) \cdot a(k_y)$$

(10)

where h_m is the windowing function (if any) used during the SAR focusing, and a is the antenna function that can be modeled (or extracted from AUX_CAL file) as a series of $\mathrm{sinc}^4(y)$ functions. The Fourier profile in range direction is established empirically by computing Fourier spectra of the complex image (Doppler shifted), and then the range Fourier profile by integrating out the azimuth dependency:

$$X(k_x) := \left\langle \frac{X(k_x)}{\max(X(k_x))} \right\rangle$$

(11)

where I_c is the complex image and h_w is the 2D Hanning window function. This is repeated for a large number of data and then normalized and averaged to give an estimate of instrument range transfer function:

$$X(k_x) := \left\langle \frac{X(k_x)}{\max(X(k_x))} \right\rangle$$

(12)

For ASAR WM Level 2 processing, this average profile is provided to the software in a binary file.

For S-1 this is provided as an internal auxiliary file, since it will not change once it has been established (see Section).

The individual look intensity image is now achieved as a multiplication in Fourier domain between the equalized full bandwidth complex SAR image and the azimuth bandpass filter, W (rectangular), followed by an inverse Fourier transform and an intensity detection. First the complex individual look image in Fourier domain, $I_c(\underline{k},t)$ is generated as:

$$I_c(\underline{k},t) = W\left(k_y + \frac{2k_{rad}V}{R}t\right) \cdot I_c(\underline{k})$$

(13)

Here

$$I_c(\underline{k}) := \frac{I_c(\underline{k})}{X(k_x) \cdot Y(k_y)}$$ = equalized Fourier transform of the full bandwidth SLC image

W = rectangular bandpass filter with amplitude 1

t = sub-look azimuth time [s]

$\underline{k} = (k_x, k_y)$ = wavenumber domain (range, azimuth) [rad/m]

R = slant range distance [m]

k_{rad} = radar wavenumber [rad/m]

Then the individual look intensity image is computed in spatial domain by an inverse Fourier transform of $I_c(\underline{k},t)$ followed by an intensity detection:

$$I^{(m)}(\underline{x}) = \left| \frac{1}{(2\pi)^2} \int d\underline{k}\, I_c(\underline{k},t) e^{-i\underline{k}\cdot\underline{x}} \right|^2, \qquad m \in [1,2,3]$$

(14)

where m represents the three different azimuth time intervals (or frequency bands) from which the intensity images are generated. In the above processing three look intensity images are generated, with configurable look separation frequency of Δf and look filter width of ΔF. Default values are given by the auxiliary data as specified in 0 of Section [7.1.2]. In range direction one look is used with a configurable bandwidth as specified in Table 1 of Section 7.1.2. Figure 4 shows the three look filters within the azimuth bandwidth.
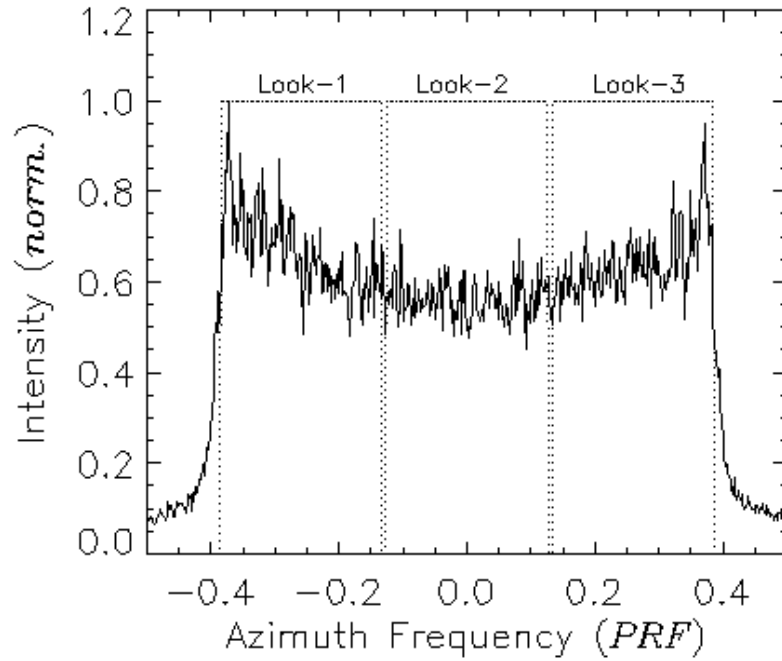
Figure 4 : Azimuth Fourier domain and the look-extraction filters.

Step 6: Estimation of Co- and Cross-Variance Function

Input Data: Three Individual Look Intensity Images $(I^{(m)}, m = 1,2,3)$, AUX_PP2 parameters, Internal Processing Parameters

Output Data: Co- and Cross-Variance function on cartesian grid ($(\rho^{(n,m)}, (m,n) \in [1,2,3])$)

The procedure is identical to what is implemented and described for ASAR WM [**Erreur ! Source du renvoi introuvable.**]. The co- and cross-variance function are the inverse Fourier transforms of the co- and cross-spectra given as:

$$\rho^{(m,n)}(\underline{x}, \Delta t) = \frac{1}{(2\pi)^2} \int d\underline{k} \, P_s^{(m,n)}(\underline{k}, \Delta t) e^{-i\underline{k}\cdot\underline{x}}, n \in [1,2,3], m \in [1,2,3]$$

(15)

where   are the co- and cross-spectra computed from the individual look intensity images of Eq.(14) as follows:

$$P_s^{(m,n)}(\underline{k}, \Delta t) = \frac{1}{\langle I^{(m)} \rangle \langle I^{(n)} \rangle} \left\langle I^{(m)}\left(\underline{k}, \frac{t}{2}\right) I^{(n)*}\left(\underline{k}, -\frac{t}{2}\right) \right\rangle - \delta(\underline{k})$$

(16)

where

$\langle I^n \rangle$ = mean image intensity

$I^{(n)}\left(\underline{k}, t/2\right)$ = Fourier transform of the look intensity image n given in Eq.(14).

$\Delta t = t/2 - (-t/2)$ = look separation time between the look intensity images, n and m,

The look separation time is related to the neigbour look separation frequency, Δf, and for neigbour looks the look separation time, is given as:

$$\tau = \frac{\pi R \Delta f}{k_{rad} V^2}$$

(17)

where

R/V = radar range to velocity ratio [s]

k_{rad} = radar wavenumber [rad/m]

Δf = configurable look separation frequency [Hz] (Table 1)

The standard deviation of the co- and cross-spectra among the periodograms is also computed as follows:

$$D_S^{(m,n)}\left(\underline{k}, \Delta t\right) = \frac{1}{\langle I^{(m)}\rangle\langle I^{(n)}\rangle} \sqrt{\left\langle\left(I^{(m)}\left(\underline{k}, \frac{t}{2}\right)I^{(n)*}\left(\underline{k}, -\frac{t}{2}\right) - \langle I^{(m)}\left(\underline{k}, \frac{t}{2}\right)I^{(n)*}\left(\underline{k}, -\frac{t}{2}\right)\rangle\right)^2\right\rangle}$$

The co-variance function is achieved by setting $m = n$ in Eq.(15), and in that case $\Delta t = 0$. The <> in Eq.(16) denotes ensemble averaging, which here is achieved by a Hanning window periodogram (50% overlap) averaging of 9×5 periodograms pr. imagette. The number of periodograms depends on the size of the imagette and the size of the periodograms. The latter depends again on the ratio of the range and azimuth look bandwidths to the range sampling and pulse repetition frequencies, respectively. A detail description how this is done can be found in the ASAR WM SRD (p.39-40) [A-7].

The spectral bin sizes are computed from the resampled ground range and azimuth resolution as:

$$\Delta k_x = \frac{4\pi 2^{\rho_x} f_{sf} \sin\theta}{N_x c}, \quad \Delta k_y = \frac{4\pi 2^{\rho_y} f_{prf}}{N_y V_g}$$

(18)

where the resampling integer powers, ρ_x and ρ_y are given as

$2^{\rho_x} \geq 2 f_x / f_{sf}, 2^{\rho_y} \geq 2 f_y / f_{prf}$.

Here

f_{sf}	= range bandwidth [Hz],
f_{prf}	= pulse repetition frequency [Hz],
f_x	= range look bandwidth (configurable) [Hz], (Table 1)
f_y	= azimuth look bandwidth (configurable) [Hz], (Table 1)
N_x	= number of range pixels (configurable, 0) in the cartesian spectra,
N_y	= number of azimuth pixels (configurable, 0) in the cartesian spectra,
θ	= incidence angle,
c	= speed of light,
V_g	= radar ground velocity.

Examples of co- and cross-variance functions are shown in Figure 5. The upper left plot is the cross-variance between look 1 and look 3. The upper right plot is the average cross-variance between look 1 and look 2, and look 2 and look 3. The lower plot is average co-spectra from look 1, look 2 and look 3. Note the small shift of the peak of the cross-variance function from the origin showing the propagation of the detected waves.
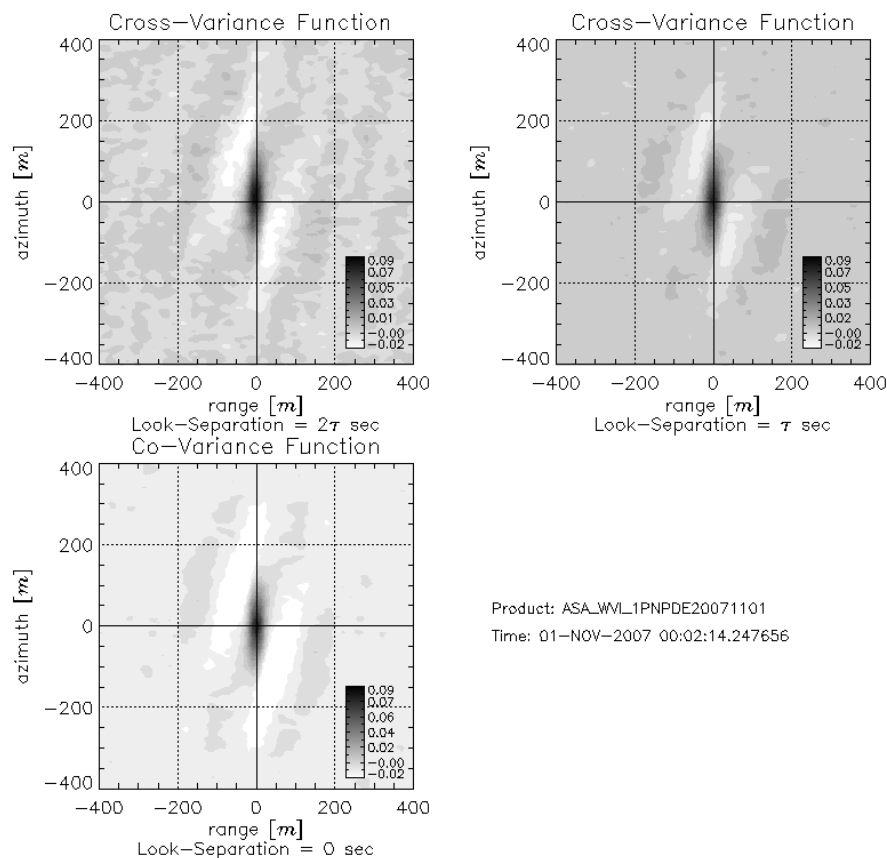
Figure 5 : Example of co- and cross-variance function processed from ASAR WM data.

Step 7: Intermediate Cross-Spectra Product

The OSW processing system has an option to store the intermediate co- and cross-variance function, image statistics, and land flag on as a disk file on an internal format. However, this option will not be used during the operational L2 processing at the IPF, instead the parameters will be kept in memory.

6.2. OSW – Spectral Inversion Unit

The spectral inversion unit transforms the co- and cross-variance functions into co- and cross-spectra followed by and inversion into an estimate of the ocean swell wave spectra. The theoretical basis for inversion unit is the same as used in the ASAR WM Level 2 processing [A-7] but upgraded with some modules from the ASAR IM and ERS wave retrieval system of SOPRANOS [A-8].

6.2.1. Flowchart

Figure 6 shows the flowchart of the OSW inversion unit.
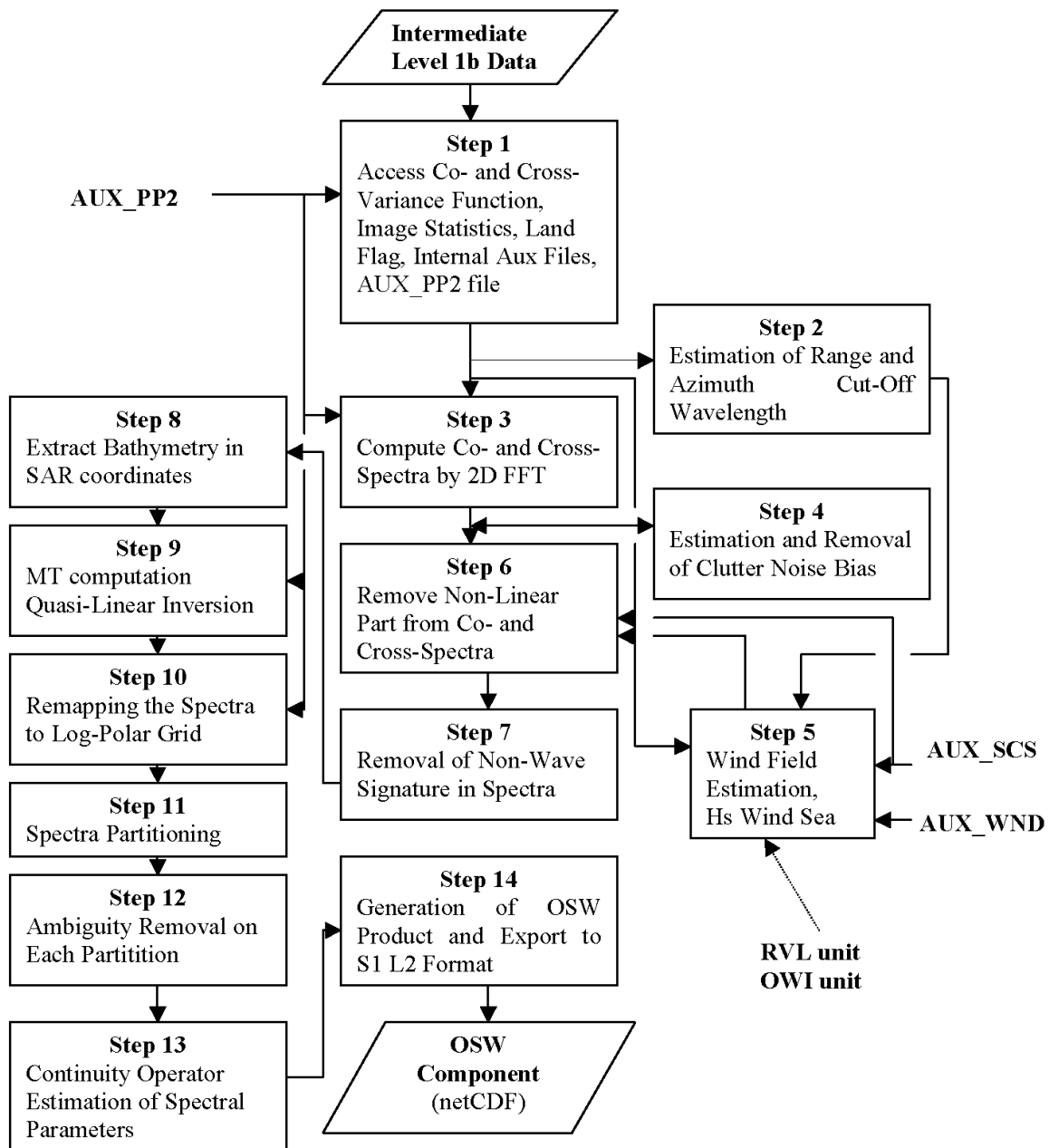
Figure 6 : Flowchart of Sentinel-1 OSW processing unit showing the main processing steps.

6.2.2. Function and Purpose

Step 1: Access the Co- and Cross-Variance Functions, Internal Processing Parameter File, and AUX_PP2 file

Input Data: Co- and Cross-Variance function ($\rho^{(n,m)}, (m,n) \in [1,2,3]$), Image statistics, Land Flag , AUX_PP2 file, Internal Processing Parameters

Output Data: Co- and Cross-Variance function on cartesian grid, and processing parameters for spectra estimation ($\rho^{(n,m)}, (m,n) \in [1,2,3]$), image statistics (Mean, Variance, Skewness, Curtosis), and Land Flag.

The co- and cross-variance data will be accessed internally, and the processing parameter information (see 0 Section [7.1.2]) and the internal processing parameter (0, Section 7.2.4) will be accessed from the processor auxiliary data and the internal parameter file, respectively.

Step 2: Estimation of Cut-Off Wavelengths and Spectral Resolution

Input Data: Co- and Cross-Variance function ($\rho^{(n,m)}, (m,n) \in [1,2,3]$), Internal Processing Parameters

Output Data: Azimuth cut-off wavelength (λ_c), range cut-off wavelength (λ_{range}), spectral resolution as function of wave direction (λ), non-linear spectra width (λ_{nl})

The azimuth and the range cut-off lengths define the spectral resolution. Since these are very different, the direction of wave propagation is important for whether the wave is detected or not. We shall therefore describe the azimuth and range cut-off and the then the spectral resolution.

<u>Azimuth Cut-Off Wavelength:</u>

The azimuth cut-off wavelength, λ_c is estimated from the normalized azimuth profile of the estimated cross-covariance function, $\rho^{(m,n)}(y) \Big/ \max\left(\rho^{(m,n)}(y)\right)$ by minimizing the functional:

$$\Delta\varepsilon = \int dy \left\{ \rho^{(m,n)}(y) - e^{-\left(\pi y / \lambda_c\right)^2} \right\}, \qquad m \neq n$$

(19)

with respect to the azimuth cut-off wavelength.

The azimuth profile, $\rho^{(m,n)}(y)$, is computed from the cross-variance function of Eq.(15) by averaging in the range direction:

$$\rho^{(m,n)}(y) = \int dx \, \rho^{(m,n)}(\underline{x},t), \qquad m \neq n$$

(20)

An alternative approach to improve the above estimator in case of azimuth traveling waves consists in maximizing the following function with respect to λ_c:

$$\Delta\varepsilon = \int dy \left\{ \frac{\partial\rho^{(m,n)}(y)}{\partial y} \cdot \frac{\partial e^{-\left(\pi y / \lambda_c\right)^2}}{\partial y} \right\}, \qquad m \neq n$$

(21)

The minimization of Eq.(19) or the maximization of Eq.**Erreur ! Source du renvoi introuvable.** are implemented using the bisection algorithm. Example of output of azimuth cut-off estimation is
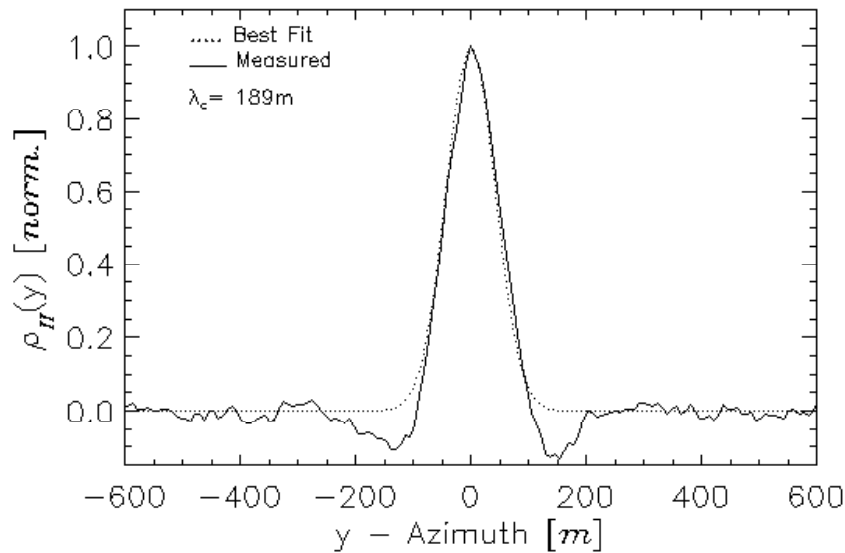
shown Figure 7.

Figure 7 : Azimuth profile of cross-variance function (___), and the best fit exponential roll-off function (.....) achieved with a cut-off wavelength of 189 m.

Range Cut-Off Wavelength:

In range, the theoretical limit is given by the ground range resolution, and it is thus dependent on the incidence angle, θ. The range cut-off wavelength is computed as:

$$\lambda_{range}(\theta) = \frac{c}{f_{sf} \sin \theta}$$

(22)

in units of meter.

Non-Linear Spectral Width:

The width of the quasi-linear image spectra is related to the azimuth cut-off length, while the width of the non-linear SAR image spectra can be related to a parameter called the non-linear spectral width, λ_{nl} [m]. This parameter can be estimated by fitting the tail of the azimuth spectral profile to a functional form, $\propto \left(k_y \frac{\lambda_{nl}}{2\pi} \right)^{-4}$ with respect to λ_{nl}, through minimization of the function:

$$\Delta \varepsilon = \int\limits_{k_y > k_c} dk_y \left| P(k_y) - \left(k_y \frac{\lambda_{nl}}{2\pi} \right)^{-4} \right|^2$$

(23)

where

k_y = the azimuth wavenumber [rad/m]

$P(k_y)$ = Fourier transform of co-variance profile $\rho^{(m,n)}(y)$, $m \neq n$

k_c = transition wavenumber

The transition wavenumber is found as the wavenumber where the azimuth spectral profile starts to follow the k_y^{-4} law.

Spectral Resolution:

The spectral resolution as function of wave direction is now computed from the azimuth and range cut-off wavelengths. The spectral resolution is an array of wavelengths equal to the number of directional bins.

We can compute the resolution [m] as function of wave direction, ϕ, relative to North using the azimuth cut-off wavelength and the along track satellite heading:

$$\text{(24)} \qquad \lambda(\phi) = \left(\lambda_c \cdot \cos(\phi + \varphi_{track}) \right) > \lambda_{range}$$

where

φ_{track} = along track heading of the satellite relative to north [deg]

λ_{range} = shortest detectable wavelength [m] in the range direction as given by Eq.(22)

The directional dependent resolution, as given by Eq.(24), helps the users interpret the OSW product.

Step 3: Computation of Co- and Cross-Spectra

Input Data: Co- and Cross-Variance function on cartesian grid ($\rho^{(n,m)}, (m,n) \in [1,2,3]$), AUX_PP2 Parameters, Internal Processing Parameters

Output Data: Co- and Cross-Spectra on cartesian grid ($P_s^{(m,n)}, (m,n) \in [1,2,3]$), Quality cross-spectra on polar grid (S_x). Look separation time (τ)

The co- and cross-spectra on cartesian grid are computed as the Fourier transform of the co- and cross-variance functions multiplied with a power, β of the Hanning window, h:

$$\text{(25)} \qquad P_s^{(m,n)}(\underline{k}) = \int d\underline{k} \, h(\underline{x})^\beta \rho^{(m,n)}(\underline{x}) e^{i\underline{k}\cdot\underline{x}} \qquad n \in [1,2,3], m \in [1,2,3]$$

The β parameter is specified in the internal processing parameter file (Table 3). Example of co- and cross-spectra are shown in Figure 8. The upper plot is the cross-spectra between look 1 and look 2. The mid plot is the cross spectra between look 1 and look 2, and between look 2 and look 3, averaged together. The lower plot is the average co-spectra of look 1 and look 2 and look 3. The cross-spectra with largest look separation time will be transformed into log-polar grid following the same approach as used in Step 10. The spectra will be embedded into the L2 OCN product as the quality cross-spectra, S_x together with the corresponding look separation time computed from Eq.(17).
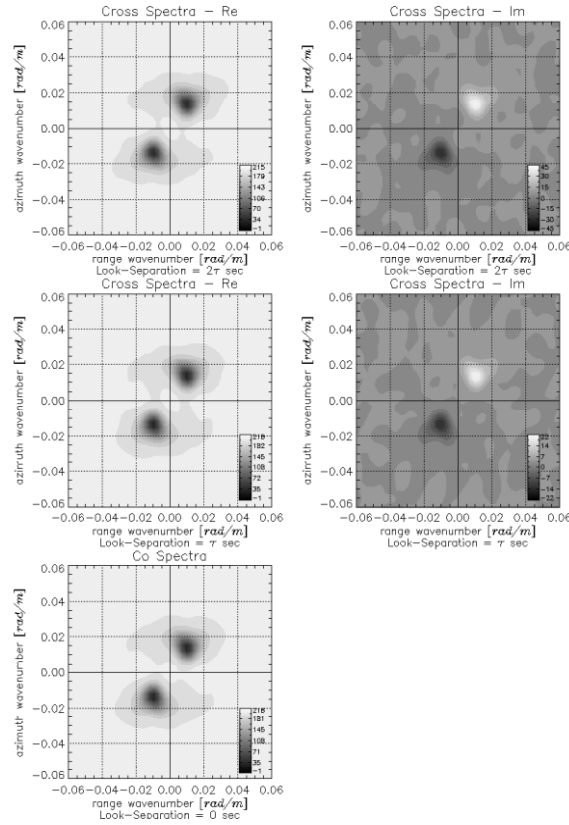
Figure 8 : Example of cross- and co-spectra processed from ASAR WM data.

Step 4: Clutter Bias Estimation and Removal

Input Data: Co-spectra on Cartesian grid ($P_s^{(m,n)}$, $m = n$)

Output Data: Co-spectra compensated for clutter bias ($P^{(m,n)}$, $m = n$)

The image spectra or variance function with zero time lag (i.e. the co-spectra, or co-variance function) will inherently be biased by speckle noise, which is not the case for the cross-spectra because the small scale statistics of the complex SAR look images can be assumed Gaussian. In order to be able to combine the co- and the cross-spectra in the inversion process, the speckle bias in the co-spectra must be removed properly. This procedure is described in the following.

The clutter bias removal is performed in the wavenumber (k) domain. The connection between the speckle biased image co-spectra, $P_s^{(m,n)}(\underline{k})$, $m = n$ and the corresponding unbiased co-spectra, $P^{(m,n)}(\underline{k})$ can be written as [**Erreur ! Source du renvoi introuvable.**]:

$$P_s^{(m,n)}(\underline{k}) = P^{(m,n)}(\underline{k}) + B(\underline{k}) = P^{(m,n)}(\underline{k}) + \int dk' \, T\left(|k_x| + |k_x'|, |k_y| + |k_y'|\right) \frac{P^{(m,n)}(\underline{k}')}{F(\underline{k}')}, \quad m = n$$

(26)

where T is the transfer function coming from the convolution of the Fourier look-extraction filter (rectangular window), and where

$$F(\underline{k}) = \int dk' \, T\left(|k_x| + |k_x'|, |k_y| + |k_y'|\right)$$

(27)

The second term of Eq.(26) is the clutter bias term, which can be estimated using the symmetry properties of this term and F in an iteration procedure **[A-7Erreur ! Source du renvoi introuvable.]**. The unspeckled spectra is then simply given by subtraction:

$$(28) \qquad P^{(m,n)}(\underline{k}) = P_s^{(m,n)}(\underline{k}) - B(\underline{k}), \quad m = n$$

For $m \neq n$ the speckle bias is zero because the decorrelation of the ocean surface scatterer is shorter than the look separation, and we simply have:

$$(29) \qquad P^{(m,n)}(\underline{k}) = P_s^{(m,n)}(\underline{k}), \quad m \neq n$$

Example of speckle bias removal from co-spectra is shown in **Erreur ! Source du renvoi introuvable.**
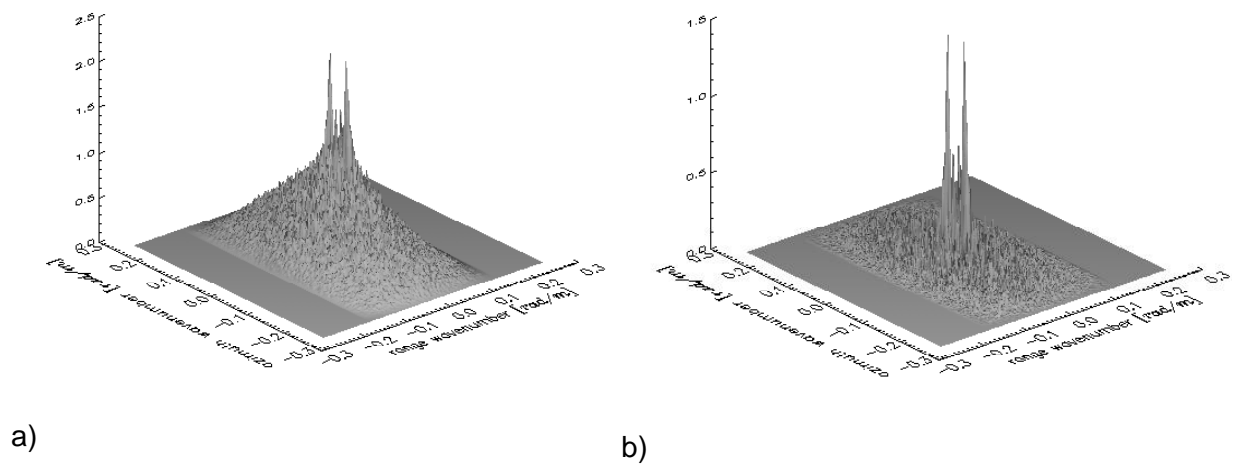
Figure 9 : Estimated SAR image co-spectra (a) and the corresponding speckle bias free co-spectra (b).

Step 5: Estimation of Wind Speed and Wind Sea Waveheight

Input Data: NRCS (σ_o), azimuth cut-off (λ_c), AUX_WND file, AUX_SCS file

Output Data: Wind vector ($\underline{U}$), wind sea waveheight ($H_s^{windSea}$) , inverse wave age (υ)

For WM the wind speed is estimated by combining the measured radar cross-section with the radar cross-section of the CMOD5n model function (for IPF 3.30 and later, previously Cmod-Ifr2) extended with a geophysical based polarization ratio model assuming the wind direction is given apriori. The geophysical model function is given by [R-10]:

$$(30) \qquad \sigma_o^{\alpha\alpha}(\theta,\underline{U}) = \sigma_{c\,\mathrm{mod}}(\theta,\underline{U}) \cdot \frac{\sigma_{gcm}^{\alpha\alpha}(\theta,\underline{U})}{\sigma_{gcm}^{vv}(\theta,\underline{U})}, \qquad \alpha\alpha \in [vv, hh]$$

where $\sigma_{c\,\mathrm{mod}}$ is the CMOD5n function and σ_{gcm} is the GCM function **[R-10]**. The polarization ratio model used is a model that incorporates both wind speed and wind direction dependency [R-10]. The model can be written on a polynomial form as:

(31)
$$\frac{\sigma_{gcm}^{hh}}{\sigma_{gcm}^{vv}} = c_o + c_1 \cos\varphi + c_2 \cos 2\varphi$$

where φ is the wind direction relative to range and where $c_i = c_i(U,\theta)$ are polynomial coefficients dependent on wind speed, U and incidence angle, θ. These coefficients are included in the software. Other models for the polarization ratios may also be used. For SM data and WV (only for IPF 3.30 and latter), the the wind speed is estimated using the above backscattering model in a bayesian algorithm. A detailed description of this algorithm (OWI processing unit) is given [**A-9**]. The ECMWF wind field is extracted from the auxiliary data file (see 7.1.1).

The wind sea significant waveheight, $H_s^{windSea}$ is estimated by using the derived wind speed, U and the estimated azimuth cut-off wavelength, λ_c as input to a precomputed functional relation (see Figure 10). This relation (coefficients) is included in the software.

(32)
$$H_s^{windSea} = f\left(\lambda_c, |U|\right)$$
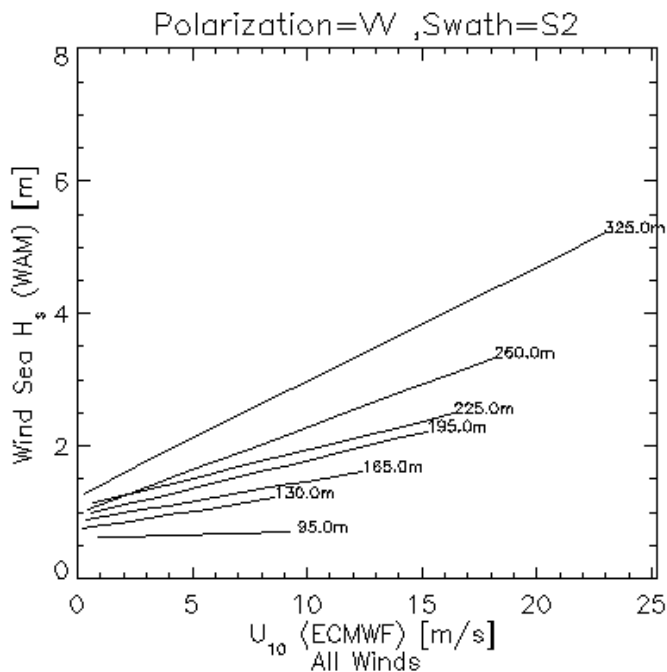
Figure 10 : Example of content of the wind sea significant waveheigth functional relation. The numbers attached to each line are the measured SAR azimuth cut-off wavelength.

The λ_c can either be estimated as described in Step 2 or provided by the RVL processing unit [**A-10**]. The wave age, υ can now be extracted from the simulated cross-spectra look-up table described in (Section 7.1.3) by interpolation using the wind speed, wind direction and wind sea waveheight.

Step 6: Removal of Non-Linear Part and Clutter Noise Estimation

Input Data: Co- and Cross-Spectra ($P^{(m,n)}, (m,n) \in [1,2,3]$), AUX_SCS file, Wind Vector ($\underline{U}$), Inverse Wave Age (υ)

Output Data: Quasi-linear estimate of Co- and Cross Spectra ($P_{ql}(t), t \in [0, \tau, 2\tau]$), and Clutter Noise Level ($\sigma^t, t \in [0, \tau, 2\tau]$).

The clutter noise variance is computed from the co- and cross-spectra at far azimuth wavenumbers as:

$$\sigma^t = \int_{\Delta \underline{k}} \mathrm{Re}\left\{ \frac{P(\underline{k})}{U(\underline{k})} \right\}^2, \qquad t \in [0, \tau, 2\tau]$$

(33)

where $\Delta \underline{k}$ defines the spectral area from which the noise variance is computed over. The area from which the clutter is computed is specified in the internal processing parameter file (Section 7.2.4) as the *clutReg*.

The Level2 algorithm is based on the ocean-to-SAR cross-spectral transform, which is an integral transform of a product between a exponential term and a polynomial term. However, this integral transform can be split into a sum of a quasi-linear and a non-linear term. The inverison model, to be described later, is based on the quasi-linear model. We thus need to remove the non-linear part, P_{nlin} from the estimated cross-spectra, P before inversion. This is done by subtraction as follows:

$$P_{qlin}(\underline{k}, t) = P(\underline{k}, t) - P_{nlin}(\underline{k}, t)$$
$$= U(\underline{k})\frac{1}{2}e^{-\left(k_y \lambda_c / 2\pi\right)^2}\left\{ |T(\underline{k})|^2 e^{-i\omega_{|\underline{k}|}t}S(\underline{k}) + |T(-\underline{k})|^2 e^{i\omega_{|\underline{k}|}t}S(-\underline{k}) \right\} \quad t \in [0, \tau, 2\tau]$$

(34)

where P_{qlin} is the quasi-linear approximation of the cross-spectra with look separation time, . We have here changed the notation from indexing m,n to (t) in the cross-spectra for describing the different spectra involved, since we now introduce a physical model for the cross spectra. Furthermore, T is the modulation transfer function, $\omega_{|\underline{k}|}$ is the dispersion relation, U is the stationary system transfer function, λ_c is the azimuth cut-off wavelength, and S is the underlying ocean wave spectra. The non-linear part, P_{nlin} is tabulated in a simulated cross-spectra look-up table as function of wind speed, wind direction and wave age. An example of P_{qlin}, P_{nlin} and P for a given wind field (i.e. underlying wave spectra) is shown in Figure 11 on a cartesian grid. The simulated cross-spectra look-up table is described in Section 7.1.3.
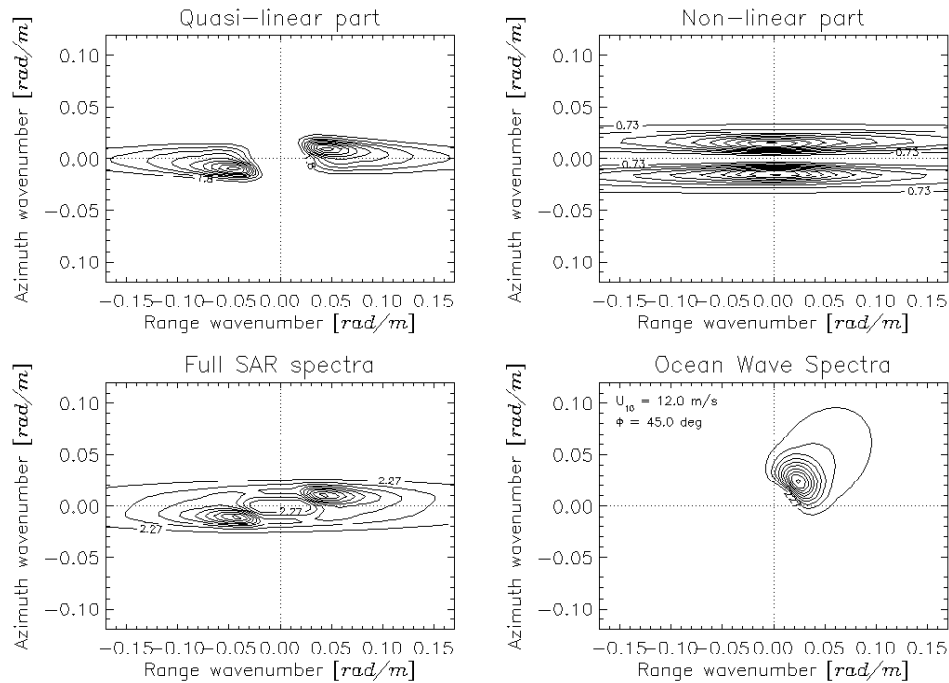
Figure 11 : Simulated cross-spectra for wind speed of 12 m/s and wind direction of 45 degrees relative to range axis. a) quasi-linear part (upper left), b) non-linear part (upper right), c) full SAR spectra (lower left), d) corresponding input ocean wave spectra (lower right).

Step 7: Removal of Non-Wave Signature

6.2.2.1.1. Input Data: Quasi-linear Co- and Cross-variance spectra ($P_{ql}(t)$, $t \in [0, \tau, 2\tau]$)

6.2.2.1.2. Output Data: Quasi-linear Co- and Cross-variance spectra filtered for low frequency non-wave signature ($P_{ql}(t)$, $t \in [0, \tau, 2\tau]$)

As often observed for ocean SAR scenes, there are numerous cases for which the measured scenes are not homogeneous in intensity. Such a phenomenon is most frequent under low wind conditions, and/or very active biological outbursts. Other phenomena that disrupt the SAR homogeneity can include internal wave signatures, rain effects, atmospheric and oceanic fronts.

The spectral signatures associated with image inhomogeneities can be very large and mostly dominate the lowest wavenumber range. To remove such undesired spectral non periodic contributions, a filtering analysis in the spectral domain is performed.
The concept is based on checking the continuity of the lowest wavenumber contributions. Indeed, wavy periodic patterns and non-wave inhomogeneities typically do not produce spectral signatures with the same continuity. Inhomogeneities will only exhibit continuously decreasing energy with increasing wavenumber while wavy patterns exhibit very sharp peaked signatures. The proposed filtering technique relies on the use of a partitioning scheme similar to the one used for the spectral partitioning of the ambiguous swell spectra described in step 11. Instead of using a classical energy descent, a watershed algorithm is used as its delineation is judged more accurate.

This partitioning includes a merging capability, aiming at merging partitions with small energy contrast. The partitioning scheme is described below:

1- The three sub-looks intensity are averaged and partitioned using a watershed algorithm
2- The neighbouring partitions with small energy contrast are merged together if:
   o The peak wavenumber of the highest peak energy partition is smaller than the input threshold (α_h parameter).

   This step is iterated until no partition can be merged.

3- The low frequency spectral domain to be removed is defined as the group of partitions with peak wavenumber smaller than α_h parameter.

The watershed algorithm is implemented using the Python library skimage.morphologys. The lowest wavenumber, α_h, from which the filtering starts from is provided in the internal processing parameter file (see 0).

This methodology has been developed and tested on Sentinel-1 Wave Mode data and is part of the new Wave Mode Level2 algorithm for wave retrieval. An example of use of the methodology is shown in Figure 12.
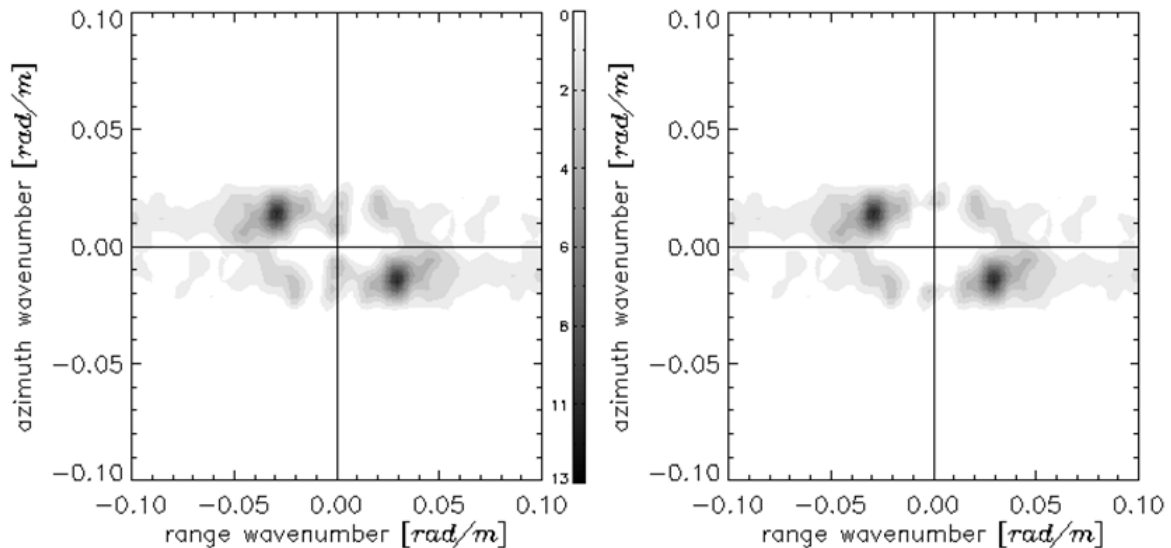
Figure 12 : (a) SAR image spectrum (real part) and before (left) and after (right) removal of low frequency non-periodic signature (b) SAR Image roughness, showing particularly low wind conditions

Step 8: Extraction of of Bathymetry Data

Input Data: LOP_GEB file

Output Data: Ocean depth (d)

If the keyword for use of bathymetry data is set in the internal parameter file (0), bathymetry within the same geographic area as the imagette is extracted from the GEBCO Gridded Bathymetry data file (Section 7.2.2), and the average depth is computed within this area.

Step 9: Computation of MTF and Spectral Inversion

Input Data: Quasi linear Co- and Cross-Spectra ($P_{ql}(t), t \in [0, \tau, 2\tau]$), AUX_SCS file, AUX_PP2 Parameters, Internal Processing Parameters, Wind Vector ($\underline{U}$), Inverse Wave Age , (γ), Azimuth Cut-Off wavelength (λ_c), Clutter Noise Variance ($\sigma^t, t \in [0, \tau, 2\tau]$), NRCS   ($\sigma_o$), Ocean Depth ($d$)

Output Data: Symmetric (S_s) and anti-symmetric (S_a) wave spectra on cartesian grid,

The total geophysical modulation transfer function (MTF) used in the inversion is given by:

$$(35) \qquad T(\underline{k}) = ik_y T_\xi(\underline{k}) + T_\sigma^{\alpha\alpha}(\underline{k})$$

where T_ξ is the shift MTF defined by:

$$(36) \qquad T_\xi(\underline{k}) = \frac{R}{V} \omega_{|k|} \left| \frac{k_x}{|\underline{k}|} \sin\theta + i\cos\theta \right| \left[1 - (\sigma + v_h) < 0 \right] / u_h$$

where v_h, u_h are provided by the internal processing parameter file (see 0) and $T_\sigma^{\alpha\alpha}$ is the RAR MTF defined by:

$$T_\sigma^{\alpha\alpha}(\underline{k}) = 2 k_{rad} k_x \nabla \sigma_o^{\alpha\alpha}(\theta, \underline{U}) \left\{ \frac{k_x}{|\underline{k}|} \sin\theta + i\cos\theta \right\}$$

$$(37) \qquad \nabla \sigma_o^{\alpha\alpha}(\theta, \underline{U}) \equiv \frac{\partial \sigma_o^{\alpha\alpha}(\theta, \underline{U})}{\partial \theta} \frac{1}{\sigma_o^{\alpha\alpha}(\theta, \underline{U})} \frac{1}{2 k_{rad} \cos\theta} \cdot \gamma(\theta, \underline{U})$$

Here:

k_{rad}	= radar wavenumber
θ	= radar incidence angle
$\omega_{|k|} = \sqrt{g|\underline{k}|\tanh(|\underline{k}|d)}$	= dispersion relation of ocean waves in finite depth
d	= water depth
R	= satellite slant range –
V	= satellite velocity
k_x	= range wavenumber
k_y	= azimuth wavenumbers
$\gamma(\theta, \underline{U})$	= correction factor for the wind dependency in the RAR MTF.

Here $\nabla \sigma_o^{\alpha\alpha}$ is tabulated in the same simulated cross-spectra look-up table as the P_{nlin} (Section 7.1.3). Knowing the modulation transfer function, Eq.(34) allows us to derive the symmetric (ambiguous) , $S_s(\underline{k})$ and the anti-symmetric (unambiguous) part $S_a(\underline{k})$, of the wave spectra:

$$S_s(\underline{k}) = \frac{1}{\sum_t 1/\sigma^t} \sum_t \frac{1}{T_m(\underline{k})} \left\{ \frac{\mathrm{Re}\{P_{qlin}(\underline{k},t)\}}{\sigma^t \cos(\omega_{|\underline{k}|}t)} \right\}, \qquad t \in [0,\tau,2\tau]$$

$$S_a(\underline{k}) = \frac{1}{\sum_t 1/\sigma^t} \frac{1}{T_m(\underline{k})} \left\{ -\frac{\mathrm{Im}\{P_{qlin}(\underline{k},t)\}}{\sigma^t \sin(\omega_{|\underline{k}|}t)} \right\}, \qquad t \in [\tau,2\tau]$$

(38)

where T_m is the total transfer function given as:

$$T_m(\underline{k}) = e^{-\left(k_y \lambda_c/2\pi\right)^2} U(\underline{k})|T(\underline{k})|^2 \left(1 + \left(\frac{k_x}{2\pi L_{res}}\right)^4\right)^{-1}$$

(39)

where L_{res} is the effective range resolution, which can be computed from the range cut-off wavelength or provided by the internal parameter file (0). The final transfer function is then adjusted for wavelength longer than the peak wavelength (since wavelengths longer than peak wavelength are not free propagating waves) using a threshold parameter (α_{mtf}) provided by the internal parameter file (0). Here λ_c is the azimuth cut-off wavelength estimated in Step 2.

The computation of $S_s(\underline{k})$ and $S_a(\underline{k})$ above is done by a weighted summation over the different look spectra using the spectral clutter noise variance, σ^t. $S_s(\underline{k})$ and $S_a(\underline{k})$ on log-polar grid are combined in Step 12 to retrieve an unambiguous wave spectra.

Step 10: Cartesian to Log-Polar Grid Transformation

Input Data: Symmetric ($S_s(k_x,k_y)$) and Anti-symmetric ($S_a(k_x,k_y)$) Wave Spectra on cartesian grid, Clutter Noise Variance ($\sigma^t, t \in [0,\tau,2\tau]$), AUX_PP2 parameters

Output Data: Symmetric ($S_s(k,\phi)$) and anti-symmetric ($S_a(k,\phi)$) Wave Spectra on log-polar grid, polar grid (k,ϕ)

The cartesian to logarithmic polar grid transformations converts the cartesian wavenumber into into a log-polar grid, $\underline{k} = (k_x, k_y) \Rightarrow \underline{k} = (k,\phi)$. The transformation is performed using bilinear interpolation. The polar grid is given in wavenumber-direction representation clockwise relative to North. The discrete wavenumbers are logarithmically spaced such as to achieve optimal sampling of the energetic part of the SAR spectra:

(40) $k_i = \alpha^i k_{min}, \quad i = 0,...,N_k - 1$

(41) $\alpha = \left(k_{max}/k_{min}\right)^{1/N_k - 1}$

where

N_k = number of wavenumber bins

$k_{max} = 2\pi/L_{min}$ = maximum wavenumbers configurable from AUX_PP2 (Table 2)

= minimum wavenumber configurable from AUX_PP2 (Table 2)

$$k_{min} = \frac{2\pi}{L_{max}}$$ = minimum wavenumber configurable from AUX_PP2 (Table 2)

The number of wavenumber as well as max and min wavenumber, and directional bins are all configurable and specified in the AUX_PP2 file, Section (7.1.2) (Table 2).

The wavenumber bin samples then become:

(42)
$$\Delta k_i = \frac{1}{2}\left(\alpha - \alpha^{-1}\right)k_i, \quad i = 0,....,N_k - 1$$

The discrete directions are equidistantly spaced between 0 and 360 degrees clockwise from North:

(43)
$$\phi_i = i\Delta\phi + \Phi_{North} = \frac{i2\pi}{N_\phi} + \Phi_{North}, \quad i = 0,....,N_\phi - 1$$

where $\Phi_{North} = \frac{\pi}{2} + \varphi_{track}$ is the angle used to convert from SAR to geographic coordinates and φ_{track} is the satellite track angle relative to north.

The discrete polar grid bin area, A can be written as:

(44)
$$A_i = k_i\Delta k_i\Delta\phi = \frac{\pi}{N_\phi}\left(\alpha - \alpha^{-1}\right)k_i^2, \quad i = 0,....,N_k - 1$$

This polar transformation is applied to both the symmetric and anti-symmetric cartesian wave spectra. A detail description of the transformation can be found in [A-7]. The output spectra are denoted S_s, S_a, and anan example of these are shown in Figure 13.
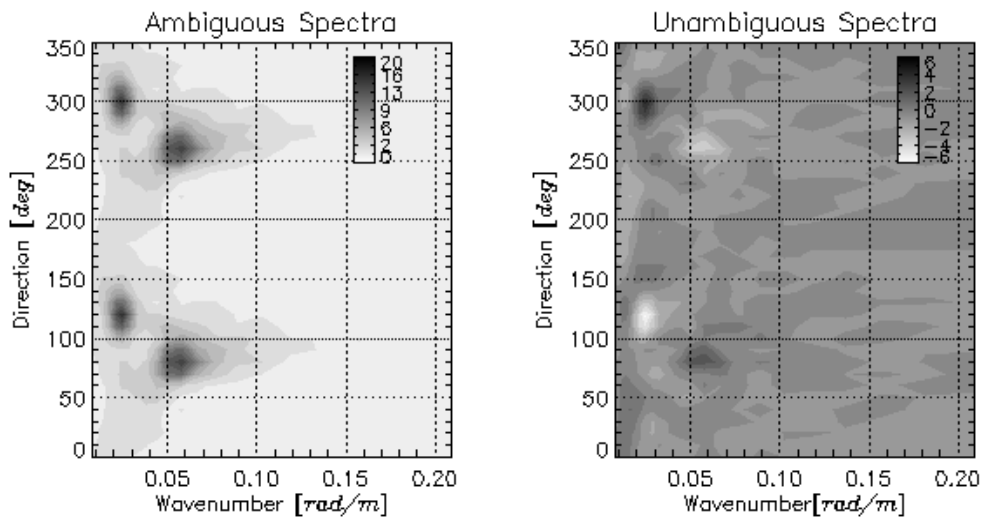
Figure 13 : Ambiguous (symmetric) (left) and unambiguous (anti-symmetric) wave spectra on log-polar (k,ϕ)-grid.

Step 11: Spectral Partitioning

Input Data: Symmetric ($S_s(k,\phi)$) and Anti-symmetric ($S_a(k,\phi)$) Wave Spectra on log-polar grid

Output Data: Partitioned symmetric $(S_s^{(p)}(k,\phi), p \in [0,1,2,3,4])$ and Anti-symmetric $(S_a^{(p)}(k,\phi), p \in [0,1,2,3,4])$ Wave Spectra (two partitions)

The spectral partitioning is applied to the polar grid representation of an ambiguous (symmetric) wave spectra. The spectral partitioning is applied with the following steps:

1. All the relative maxima above the discard_threshold (See 0) are identified in the ambiguous wave spectra. This is performed using the python library skimage.feature and the function "peak_local_max".

2. The ambiguous wave spectra is partitioned. This is performed using the python library skimage.morphology and the function "watershed".

3. The processing then entre the following iterative process:

    3.1. Connected partitioned are identified

    3.2. If the contract between two connected partitions is below a certain threshold, these partitions are merged. In practice, this threshold has been empirically set to 12 times the estimated clutter noise level.

    3.3. This process repeats until no partition can be merged anymore

4. Partitions that are related to the same wave system with opposite direction are identified and set to the same partition number.

An example of partition of a bi-modal ASAR Level 2 wave spectra is shown in **Erreur ! Source du renvoi introuvable.**. In Figure 14 a) is shown the wave spectra from using the real part of the cross-spectra, and in b) the wave spectra using the imaginary part of cross spectra. In c) and d) the spectral domains of the two most energetic partitions are shown. In Step 12 these partitions are separately used to remove the wave propagation ambiguity.

a)

b)

c)

d)

Figure 14 : a) Ambiguous (symmetric) part of OSW spectra showing bi-modal wave system. b) Unambiguous (anti-symmetric) part of OSW spectra. c) and d) partititions areas (red) and boundaries (blue) of the two wave systems after ambiguity removal using the anti-symmetric part (b).
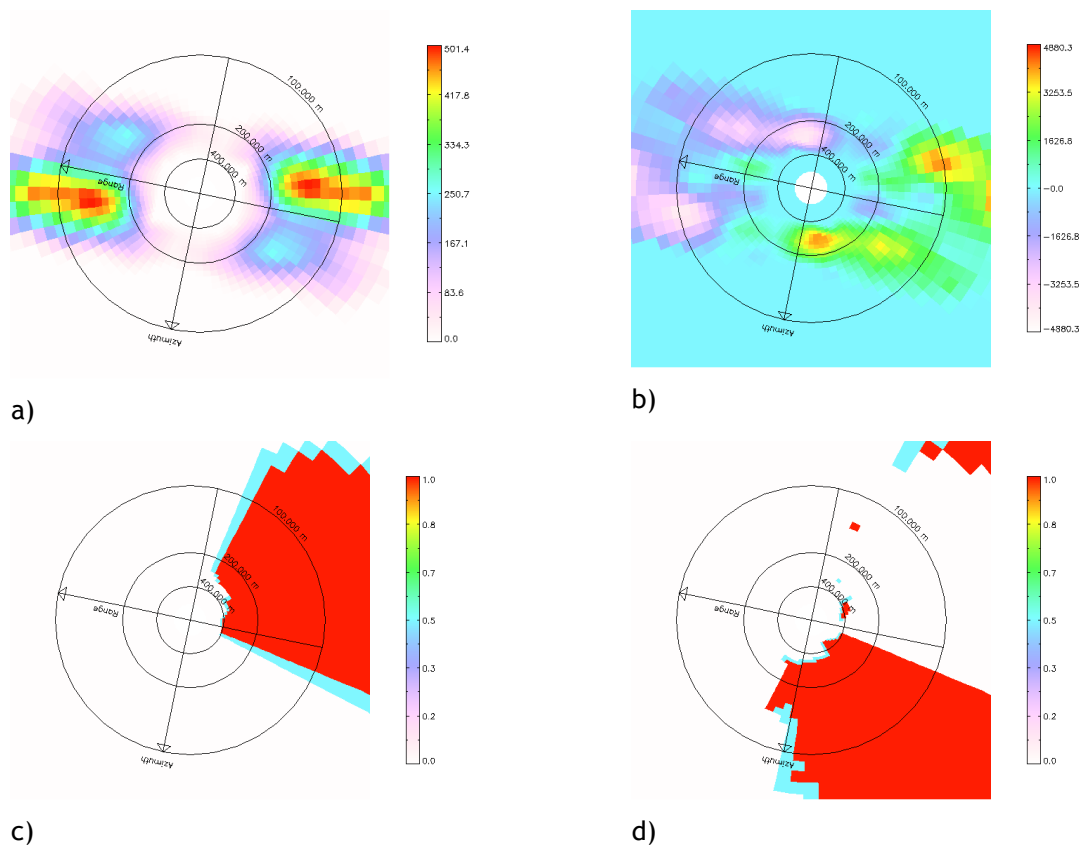
Step 12: Ambiguity Removal

6.2.2.1.3. Input Data: Partitioned symmetric ($S_s^{(p)}(k,\phi), p \in [0,1,2,3,4]$) and Anti-symmetric ($S_a^{(p)}(k,\phi), p \in [0,1,2,3,4]$) Wave Spectra

6.2.2.1.4. Output Data: Partitioned wave spectra ($S^{(p)}(k,\phi), p \in [0,1,2,3,4]$), ambiguity factor $\gamma^{(p)}, p \in [0,1,2,3,4]$)

For each partition an ambiguity factor is estimated as the integral of the corresponding unambiguous part over the considered partition weighted by the wave spectral energy over the same partition:

$$\gamma^{(p)} = \frac{\int dk \left\{ S_a^{(p)}(\underline{k}) \cdot S_s^{(p)}(\underline{k}) - S_a^{(p)}(-\underline{k}) \cdot S_s^{(p)}(-\underline{k}) \right\}}{\int dk \left\{ \left| S_s^{(p)}(\underline{k}) \right|^2 + \left| S_s^{(p)}(-\underline{k}) \right|^2 \right\}}, \qquad p \in [1,2]$$

(45)

where the index p indicate a unique partition, and $S_s^{(p)}, S_a^{(p)}$ are the symmetric and anti-symmetric wave spectra on log-polar grid for a given partition, p.

If the absolute value of the ambiguity factor exceeds a threshold, $\left| \gamma^{(p)} \right| > \gamma_{amb}$ specified in the internal processing parameter file (see 0) the ambiguity is removed and only the partition corresponding to a positive ambiguity factor is kept and multiplied by 2 for energy conservation.

In 0 a) and b) the spectral domains of the partitions are applied to the spectra of 0 a) resulting in the two wave systems. Finally, in 0 c) the two partitions are added to provide the complete wave spectra (OSW). For each partition the dominant wave spectral parameters are estimated as described in Step 13.

a)

b)

c)
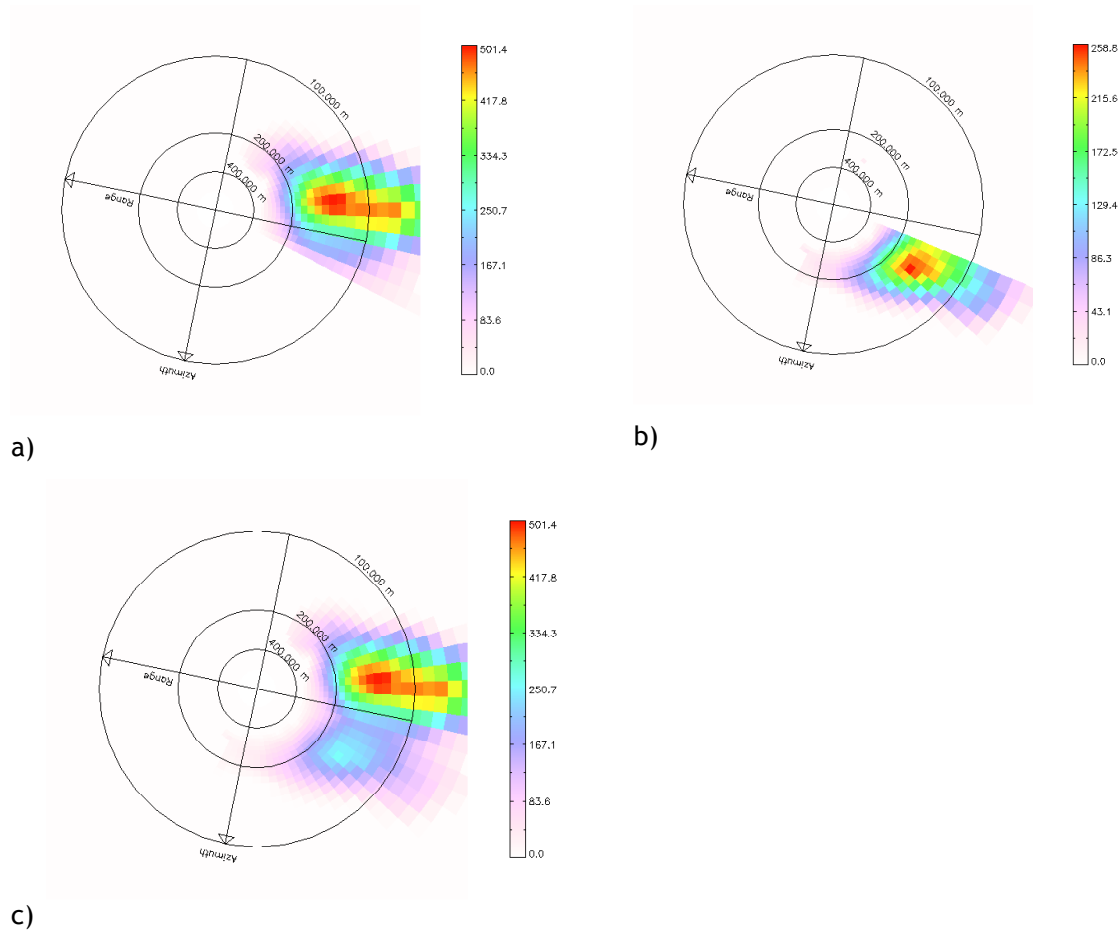
Figure 15 : a) and b) partitions of OSW spectra in two wave systems after ambiguity removal. c) final OSW spectra after merging the two partitions of a) and b).

Step 13: Estimation of Spectral Parameters

Input Data: Partitioned Wave Spectra ($S^{(p)}(k,\phi), p \in [0,1,2,3,4]$)

Output Data: Significant Waveheight ($H_s^{(p)}$), Dominant Wavelength ($\lambda_{peak}^{(p)}$), and Dominant Wave Direction ($\phi_{peak}^{(p)}$) for $p \in [0,1,2,3,4]$

Some of the most common used spectral parameters are estimated from the partitioned SAR derived ocean wave spectra. These are the peak wavelength, peak direction and significant waveheight derived for eaché of the partitions, p. The maximum number of partitions is 5. If there is some energy in the wave spectra beyond the fifth wave partition, the energy is kept in the wave spectra but no partition number is assigned.

The <u>peak wavelength</u> is given as:

$$\lambda_{peak}^{(p)} = \frac{2\pi}{k_{peak}^{(p)}}, p \in [0,1,2,3,4])$$

Where $k_{peak}^{(p)}$ is the peak wavenumber of partition p. The peak wavenumber is computed from the wave spectra as:

$$(46) \qquad k_{peak}^{(p)} = \frac{\int_{k_{max}-\Delta k}^{k_{max}+\Delta k} k S^{(p)}(k,\phi_{max})dk}{\int_{k_{max}-\Delta k}^{k_{max}+\Delta k} S^{(p)}(k,\phi_{max})dk}$$

where Δk is a 3 wavenumber interval and (k_{max}, Φ_{max}) is the location of the partition's maximum energy. The wavenumber spectra is computed from the wave spectra as:

$$(47) \qquad F^{(p)}(k) = \int S^{(p)}(k,\phi)kd\phi, \ p \in [0,1,2,3,4])$$

The <u>peak direction</u> is direction around the peak of the directional spectra. It is estimated as follows:

$$\phi_{peak}^{(p)} = \frac{\int_{\phi_{max}-\Delta\phi}^{\phi_{max}+\Delta\phi} \phi S^{(p)}(k_{max},\phi)d\phi}{\int_{\phi_{max}-\Delta\phi}^{\phi_{max}+\Delta\phi} S^{(p)}(k_{max},\phi)d\phi}, p \in [0,1,2,3,4])$$

where $\Delta\Phi$ is a 3 direction interval and (k_{max}, Φ_{max}) is the location of the partition's maximum energy. The directional spectra is computed from the wave spectra as:

$$(48) \qquad D^{(p)}(k) = \int S^{(p)}(k,\phi)kdk, \ p \in [0,1,2,3,4])$$

$(49) \qquad$ The <u>significant waveheight</u> is computed from the wave spectra as:

$$(50) \qquad H_s^{(p)} = 4\sqrt{\int S^{(p)}(k,\phi)kdkd\phi}, p \in [0,1,2,3,4])$$

Step 14: Level 2 OSW NetCDF Component

The OSW component will be stored temporarily on a disk file. When all the L2 processing units (RVL, OWI, OSW) are finished and the respective components are stored on disk, the merging of the information into the final NetCDF L2 OCN product will be done (see Section 3).

7. Input Files

This section is an overview of the auxiliary files used by OSW processing, and more information is provided in the Auxiliary Specification document **[A-3]**, the Product Specification document **[A-4]**, and Interface Control document **[A-12]**. The auxiliary file description is here separated into internal and external files. The internal files are meant not to be changed during mission, while the external files may change.

7.1. External Auxiliary Data Files

7.1.1. Atmospheric Model Wind Field – AUX_WND

Wind speed and direction at 10 m above the sea surface from the ECMWF atmospheric model is required with spatial and temporal resolution of 0.125x0.125 degrees every 3 hours. Details of the ECMWF Atmospheric Model are provided in **[A-3]**.

7.1.2. L2 Processor Parameter Auxiliary Data – AUX_PP2

The OSW processing is flexible, and the processing can be configured with the key parameters specified in the tables below.

Spectral Estimation Unit Processor Auxiliary Data:

The spectral estimation unit processor auxiliary parameters are listed in Table 3.

Table 3: OSW – Spectral Estimation Unit

Parameter	Description	Unit	Default Value
Δf	Frequency separation of neighbour looks	Hz	$0.27 f_{PRF}$
f_y	Azimuth look filter width	Hz	$0.25 f_{PRF}$
f_x	Range look filter width	Hz	$0.78 f_{sf}$
N_L	Number of individual looks	-	3
L_x, L_y	Number of slant range and azimuth pixels of L1 product used in estimation of one single OSW spectra (for WV these are equal to $\widehat{L}_x, \widehat{L}_y$ of 0.	-	Size of WV SLC

Spectral Inversion Unit Processor Auxiliary Data:

The spectral inversion unit processor auxiliary parameters are given in Table 4.

Table 4 : OSW – Spectral Inversion Unit

Parameter	Description	Unit	Default Value
L_{min}	Shortest wavelength of output polar grid	m	20
L_{max}	Longest wavelength of output polar grid	m	800
N_k	Number of wavenumber bins in polar grid	-	30
N_ϕ	Number of directional bins in polar grid	-	36

Details of the L2 Processor Parameter Auxiliary Data are provided in [**A-3**].

7.1.3. Simulated Cross-Spectra – AUX_SCS

The OSW processing algorithm requires a simulated cross-spectra look-up table to predict the modulation transfer function (MTF) and to remove non-linear effects from the cross spectra. There is one look-up table for each swath and polarisation. The basic content of the look-up table is the simulated cross-spectrum (non-linear part) for a given ocean wave spectrum, computed from the input wind speed, direction and inverse wave age, and an estimate of the MTF for the given wind field:

Output:

- The simulated cross-spectra (non-linear part) are computed on a cartesian wavenumber grid for a wide range of wind speeds and directions;

- The RAR MTF is computed on the same cartesian wavenumber grid;

Input:

- The wind speed, U range in steps of 2 m/s [2– 22 m/s];

- The wind direction φ in steps of 15 degrees [0-180 degrees];

- The inverse wave age υ in steps of 0.14 s [0.4 – 1.8].

Specification:

The baseline for the simulated cross-spectra will be what was provided for ASAR WM.

In the future a parameterisation of the simulated 2D spectra will be developed in order to save space and processing time.

Details of the Simulated Cross-Spectra Data are provided in [**A-3**].

7.2. Internal Auxiliary Data Files

7.2.1. Coastline and Land Masking Data – LOP_CLM

Wave inversion processing is not performed if land coverage is greater that 10% in the imagette considered. The land coverage is estimated as the ratio between the surface area of imagette and the surface area of a local land mask that covers the imagette. The coastline to be used should be quite accurate; an accurate shoreline polyline from the GSHHS is required. This shoreline database is available at http://www.ngdc.noaa.gov/mgg/shorelines/gshhs.html. Details of the Coastline and Land Masking data are provided in [**A-3**].

7.2.2. GEBCO Gridded Bathymetry Data – LOP_GEB

The water depth from a global bathymetry database as a pre-computed array of 1 km spatial resolution over the globe derived from the General Bathymetric Chart of the Oceans (GEBCO) http://www.gebco.net/data_and_products/gridded_bathymetry_data/. Details of the GEBCO Gridded Bathymetry data are provided in [**A-3**].

7.2.3. Range Fourier Profile – LOP_FOU

This is an average range fourier profile used to flatten the Fourier domain before look extraction. It will be estimated from data when available, and store as an internal binary file. Once established from real data, the file will not change. The file will contain (see 6.1.2) float values.

7.2.4. Internal Processing Parameter File – PRM_LOPIn

When the L2 processor receives a job order request, the L2 processor will access the processing parameters via the L2 Processor Parameter Auxiliary File (AUX_PP2 file). There is also included in the design an IPF internal parameter file for the L2 OSW processor in case more parameters than those defined in the AUX_PP2 file. These parameters are specified in the Internal Processing Parameter File, and will be used during the algorithm development phase for tuning the L2 processor performance. The parameters are specified in Table 5.

Table 5 : OSW – Internal processing parameter file

Parameter	Description	Unit	Default Value
use_bathy	Switch for use of bathymetry data (use_bathy=1)	-	0
N_x, N_y	Number of range and azimuth pixels in cartesian co- and cross-spectra	-	256,256
w	Width of low-pass filter for detrending of SLC image	m	500
use_landMask	Switch for use of land mask (landMask=1)	-	0
L_{res}	Effective range resolution used to tune RAR MTF	m	$\dfrac{c}{f_{sf} \sin \theta}$
α_h	Lowest wavenumber used in the low frequency filtering process	rad/m	$2\pi/800.$
v_h, u_h	Parameters used to tune the velocity bunching MTF	-	10,15
w	Factor used in the filter for smoothing the ambiguity spectra before partitioning	-	10
γ_{amb}	Signal-to-noise ratio threshold for ambiguity removal	-	0.05
β	Order of Hanning window function in each directions	-	2
α_{mtf}	Parameter used to tune the MTF for low wavenumbers	-	0.5
$clut\,\mathrm{Re}\,g$	Factors specifying the spectral clutter estimation region (range/azimuth sizes, azimuth position)	-	0.15,0.04,0.95
Discard_threshold	Threshold under which the energy is considered in the noise level in the wave spectra	m^4	8

7.3. SAR Product

7.3.1. SAR Image

The processing system can access and process the following SAR SLC data:

Table 6 : Input SAR SLC data

Satellite	Product Name	Format
Sentinel-1	SM SLC WV SLC	S-1 format
Envisat ASAR	IMS SLC WVI SLC	S-1 format and ASAR format
ERS SAR	IMS SLC WVI SLC	ASAR format

7.3.2. SAR product annotations

The processing requires the following data to be extracted from the SLC Level 1 product.

Table 7 : Input parameters extracted from SLC data

Parameter	Description	Unit
$\hat{L}_x, \hat{L}_y$	Number of range and azimuth pixels in the input SLC image	-
I^c	The input SLC image of size ($L_x \times L_y$)	-
f_{dc}	Azimuth doppler offset frequency	Hz
f_{prf}	Pulse repetition frequency	Hz
f_{sf}	Radar signal sampling frequency	Hz
k_{rad}	Radar wavenumber	Rad/m
F_y	Azimuth bandwidth	Hz
$\underline{S}$	State vectors $(\underline{x}, \underline{v}, t)$	m,m/s,s
K	Calibration vector, LUT	-

8. List of symbols

The following list provides the definitions of major symbols used in the document.

k_{rad}	= radar wavenumber [rad/m]
θ	= radar incidence angle [deg]
$\omega_{|\underline{k}|}$	= dispersion relation of ocean waves in finite depth [rad/s]
R	= satellite slant range [m]
V	= satellite velocity [m/s]
$\underline{k} = (k_x, k_y)$	= wavenumber vector [rad/m]] on cartesian grid
$\underline{k} = (k, \phi)$	= wavnumber vector [rad/m, degN], degN] on log-polar grid
f_{sf}	= the range bandwidth [Hz]
f_{prf}	= the pulse repetition frequency [Hz]
v_g	= the radar ground velocity [m/s]
N_x	= number of range pixels (configurable) in the cartesian spectra,
N_y	= number of azimuth pixels (configurable) in the cartesian spectra,
N_k	= number of wavenumbers (configurable) in output wave spectra,
N_ϕ	= number of directions (configurable) in output wave spectra,
φ	= wind direction relative to range [deg]
ϕ	= wave direction relative to range [deg]
τ	= look separation time [m/s]
I^c	= complex image (SLC)
I	= detected image (intensity)
ρ	= auto- and cross-correlation function
P	= co- and cross-spectra on cartesian grid
S_x	= quality cross-spectra on log polar grid
P_{qlin}	= quasi-linear part of co- and cross-spectra on cartesian grid
P_{nlin}	= non-linear part of co- and cross-spectra on cartesian grid
S	= swell wave spectra on log-polar grid [m^2]
S_a	= anti symmetric swell wave spectra on log-polar grid [m^2]
S_s	= symmetric swell wave spectra on log-polar grid [m^2]
T	= total geophysical modulation transfer function
T^ξ	= velocity shift modulation transfer function

T_σ = real aperture modulation transfer function

T_m = total modulation transfer function

$\underline{U}$ = wind vector (speed, direction) [m/s,degN]

H_s = significant waveheight [m]

υ = inverse wave age

λ_{peak} = dominant wavelength [m]

ϕ_{peak} = dominant wave direction [degN]

λ_c = azimuth cut-off wavelength [m]

λ_{range} = range cut-off wavelength [m]

$\lambda(\phi)$ = spectral resolution [m] as function of wave direction

λ_{nl} = non-linear cross spectral width [m]

σ_o = normalized radar cross section

γ = spectral ambiguity ratio

μ = mean image intensity

$\hat{\sigma}$ = normalized image variance

β_s = image skewness

β_k = image curtosis

9. OSW Output Component Contents

The following is a brief description of the OSW component content of the OCN NetCDF file. When the OSW, RVL and OWI components are generated on internal files the final OCN product will be generated by merging the information from these files into a common NetCDF file. The number in the fields may differ for the Sentinel-1 L2 product. More detailed presentation of these outputs can be found in [A4].

The OSW component of the L2 OCN annotations data set includes the following dimensions

- Number of wave cells in the range direction
- Number of wave cells in the azimuth direction
- Number of wavenumber bins in the polar spectrum
- Number of angular bins in the polar spectrum
- Number of partitions per wave cell

The OSW component of the L2 OCN data set also includes the following variables per wave cell:

- Longitude at cell centre
- Latitude at cell centre
- Two way slant range time at cell centre [sec]
- Zero Doppler time at cell centre
- Ground range size of estimation area [m]
- Azimuth size of estimation area [m]
- Incidence angle at cell centre [deg]
- Satellite heading
- Input Image Statistics
  - Image intensity
  - Nomalized image variance
  - Image skewness
  - Image kurtosis
- 2D ocean wave spectra on log-polar grid [m^4]
- 2D ocean wave partition numbers on log-polar grid
- 2D quality cross-spectra on log-polar grid [m^2]
- Array of the wavenumbers for polar spectra [rad/m]
- Array of the angular values for polar spectra [degN]
- look separation time (between inner and outer look) [s]
- Normalised radar cross section [dB]
- Significant waveheight of wind sea [m]
- Inverse wave age of wind sea
- Signal-to-noise ratio (or clutter noise variance)

- Azimuth cut-off wavelength of swell spectra [m]

- Range cut-off wavelength of swell spectra [m]

- Vector of shortest detectable wavelength for each wave direction in the swell spectra [m]

- Significant waveheight for each wave partition [m]

- Dominant wave length for each wave partition [m]

- Dominant wave direction for each wave partition [degN]

- Ambiguity ratio for each wave partition

- Confidence for each wave partition

- Auxiliary Data Derived Statistics

  - ECMWF SAR wind speed [m/s]

  - ECMWF SAR wind direction [degN]

  - Land flag for each SAR wave cell

  - Percentage of land coverage (for SM in coastal zones)

  - Water depth (for SM in coastal zones)

The OSW component of the L2 OCN data set includes the global attributes:

- Mission name

- Level 1 source filename

- Processing time

- Polarisation

- State vector

- OSW algorithm version

- Grid cell size [m^2]

Appendix A - **Acronyms and Abreviations**

ASAR	Advanced Synthetic Aperture Radar
CLM	Coast-Line and Land Masking
CLS	Collecte Localisation Satellites
CMOD4	C-band Model Function 4
CMOD-IF2	C-band Model Function Ifremer 2
dB	Decibel(s)
DC	Doppler Centroid
DCE	Doppler Centroid Estimate
ECMWF	European Centre for Medium-range Weather Forecasts
ENVISAT	ENVIronment SATellite
ERS	Earth Resource Satellite
ESA	European Space Agency
ESRIN	European Space Research Institute
EW	Extra Wide Swath
GCM	Global Climate Model
GEBCO	General Bathymetric Chart of the Oceans
GMES	Global Monitoring for Environment and Security
GMF	Geophysical Model Function
GSHHS	Global Self-consistent, Hierarchical, High-resolution Shoreline
HH	Horizontal polarisation on transmit, Horizontal polarisation on receive
IDL	Interactive Data Language
IFREMER	Institut français de recherche pour l'exploitation de la mer
IM	Image Mode (ASAR)
IPF	Instrument Processing Facility
IW	Interferometric Wide Swath
L1	Level 1
L2	Level 2
MDA	MacDonald, Dettwiler and Associates Ltd.
MET	Meteorological
MTF	Modulation Transfer Function
NESZ	Noise Equivalent Sigma Zero
NOAA	National Oceanic and Atmospheric Administration
NRCS	Normalised Radar Cross Section
NWP	Numerical Weather Prediction
OCN	L2 Ocean Product
OSC	Ocean Surface Currents

OSW	Ocean Swell Spectra Component of OCN product
OWI	Ocean Wind Field Component of OCN product
PDF	Probability Density Function
PF-ASAR	Processing Facility – Advanced Synthetic Aperture Radar
PRF	Pulse Repetition Frequency
R&D	Research and Development
RAR	Real Aperture Radar
RCS	Radar Cross Section
RMS	Root Mean Square
RMSe	Root Mean Square Error
RVL	Radial Velocity Component of OCN product
S-1	Sentinel-1
S/C	Signal-to-Clutter
SAR	Synthetic Aperture Radar
ScanSAR	Scanning SAR
SLC	Single-Look Complex
SM	Stripmap
SNR	Signal to Noise Ratio
SOPRANO	SAR Ocean Products Demonstration
SRR	System Requirements Review
TBC	To Be Confirmed
TBD	To Be Determined
TOPS	Terrain Observation with Progressive Scans
UTC	Universal Time Coordinate
V	Vertical
VV	Vertical polarisation on transmit, Vertical polarisation on receive
WAM	Wave Prediction Model
WV	Wave Mode